

# 3D Characterization of the Columnar-to-Equiaxed Transition in Additively Manufactured Inconel 718

Andrew T. Polonsky<sup>1,2</sup>, Narendran Raghavan<sup>3</sup>, McLean P. Echlin<sup>2</sup>,  
Michael M. Kirka<sup>3</sup>, Ryan R. Dehoff<sup>3</sup>, and Tresa M. Pollock<sup>2</sup>

<sup>1</sup>Sandia National Laboratories

<sup>2</sup>University of California, Santa Barbara

<sup>3</sup>Oak Ridge National Laboratory



**Sandia  
National  
Laboratories**



# Outline

- Background
- Three-dimensional Characterization
- Calibrating a Microstructure-Processing Map
- Summary

# Outline

- Background
- Three-dimensional Characterization
- Calibrating a Microstructure-Processing Map
- Summary

# Additive manufacturing (AM) provides enormous flexibility in design

## Aerospace



Images courtesy Fraunhofer IWU, Lawrence Livermore National Lab, EOS, Added Scientific, and Imperial Machine & Tool Co.

# Additive manufacturing (AM) provides enormous flexibility in design

## Aerospace



## Biomedical



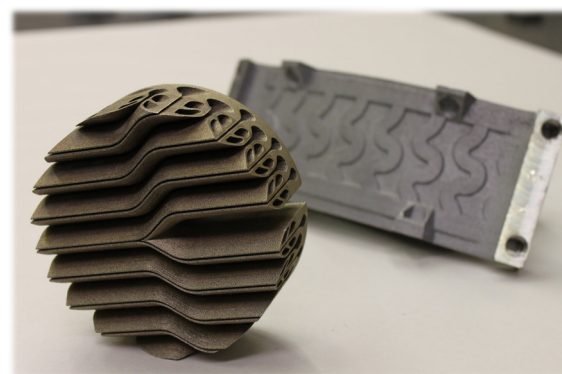
Images courtesy Fraunhofer IWU, Lawrence Livermore National Lab, EOS, Added Scientific, and Imperial Machine & Tool Co.

# Additive manufacturing (AM) provides enormous flexibility in design

## Aerospace



## Industrial



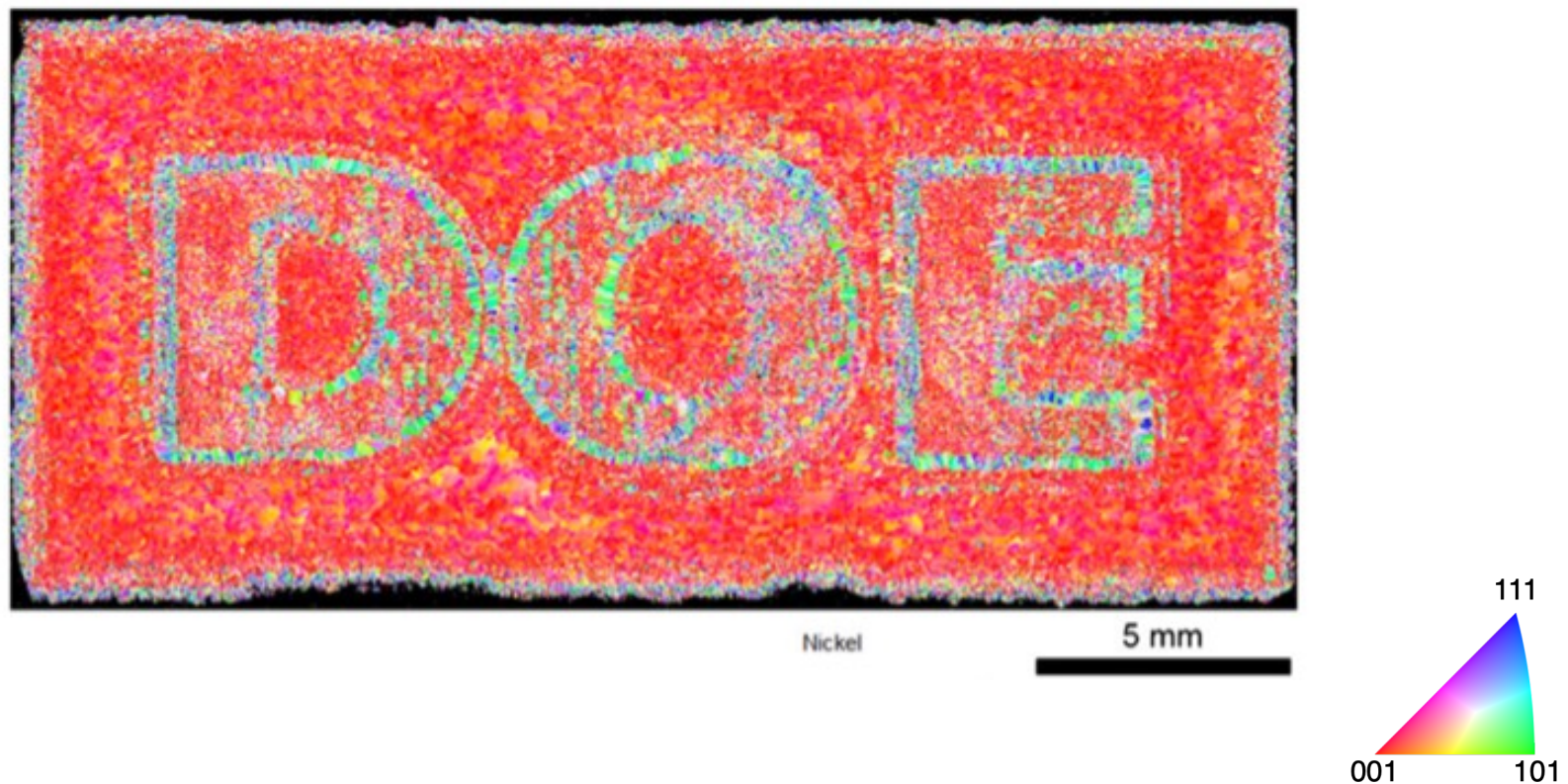
## Biomedical



Images courtesy Fraunhofer IWU, Lawrence Livermore National Lab, EOS, Added Scientific, and Imperial Machine & Tool Co.

# Scan strategy can be manipulated for site-specific microstructure

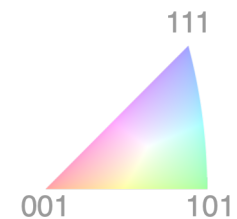
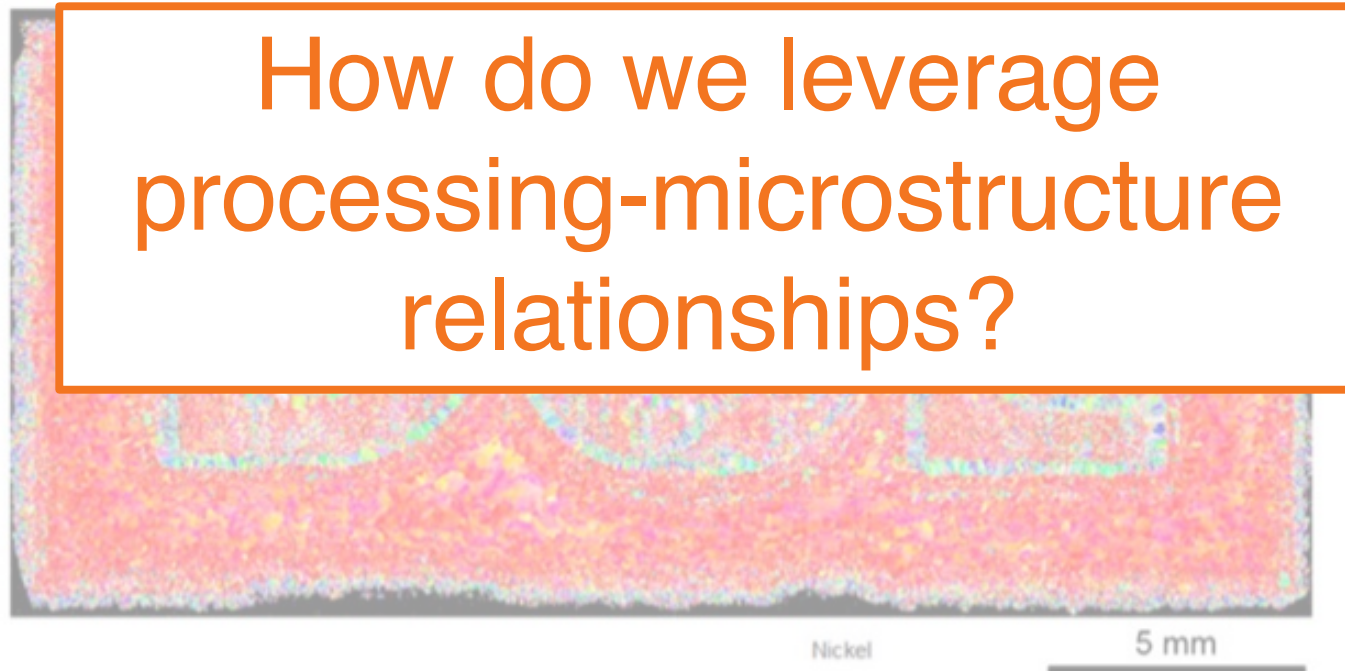
- Founded in parametric studies that are not easily generalizable to complex geometries



# Scan strategy can be manipulated for site-specific microstructure

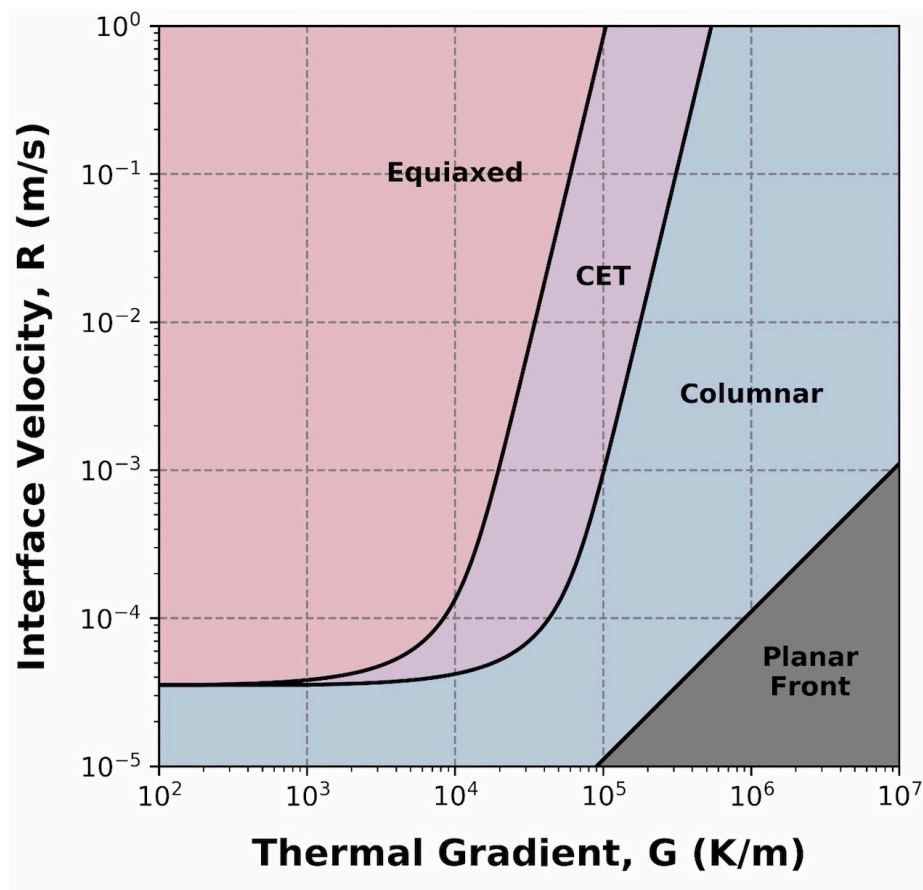
- Founded in parametric studies that are not easily generalizable to complex geometries

How do we leverage  
processing-microstructure  
relationships?



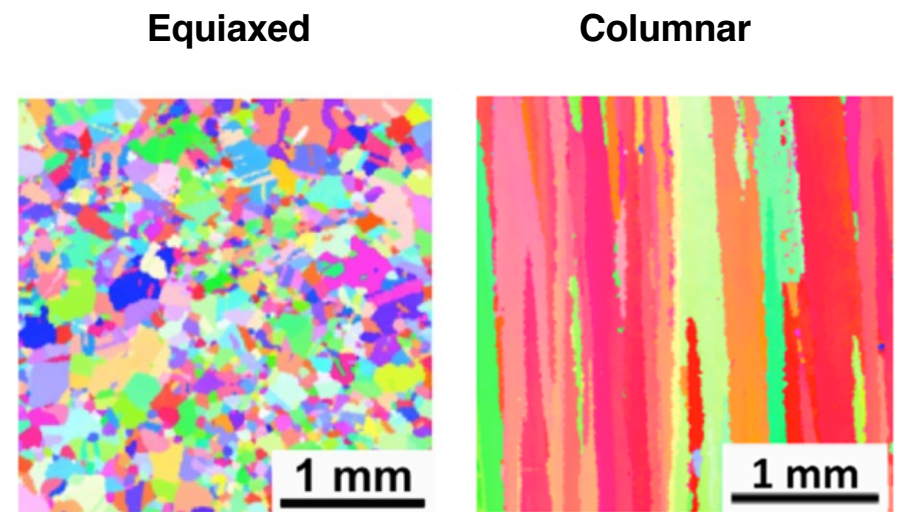
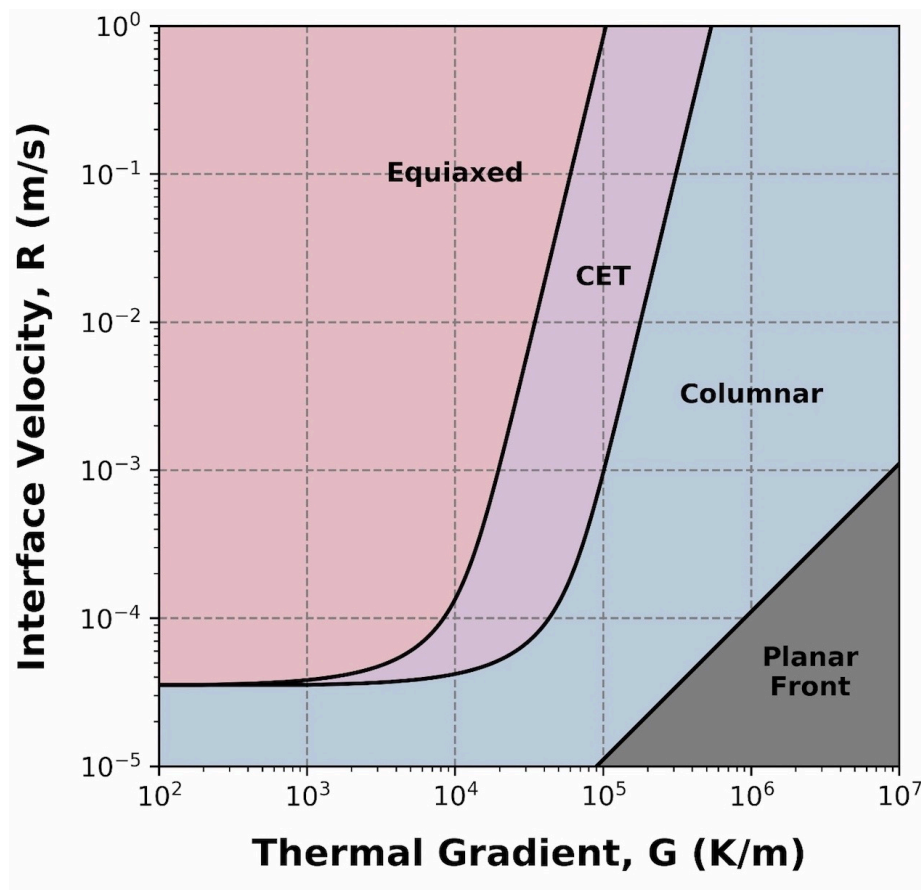
# Local microstructure control relies on understanding solidification conditions

- Processing maps help predict microstructure



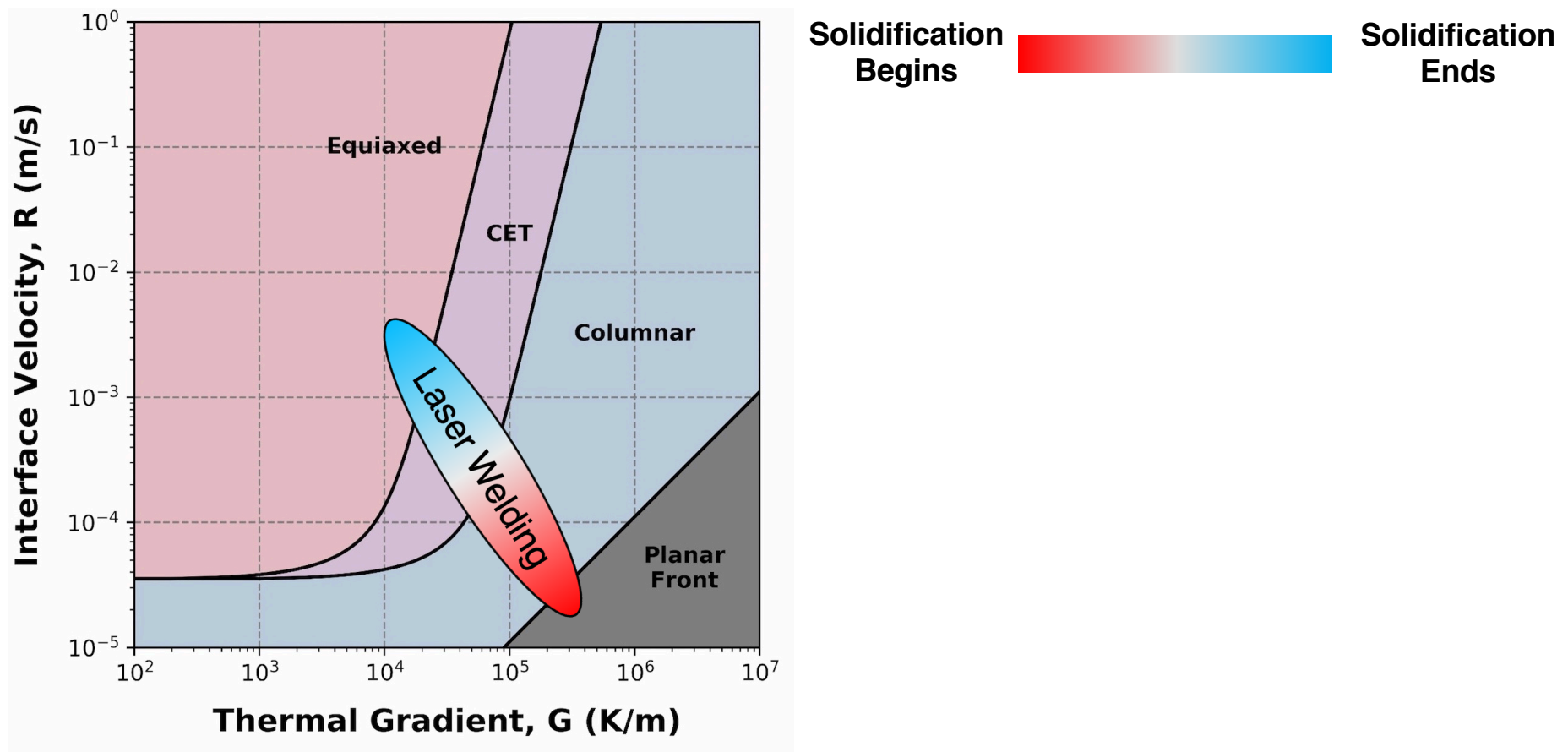
# Local microstructure control relies on understanding solidification conditions

- Processing maps help predict microstructure



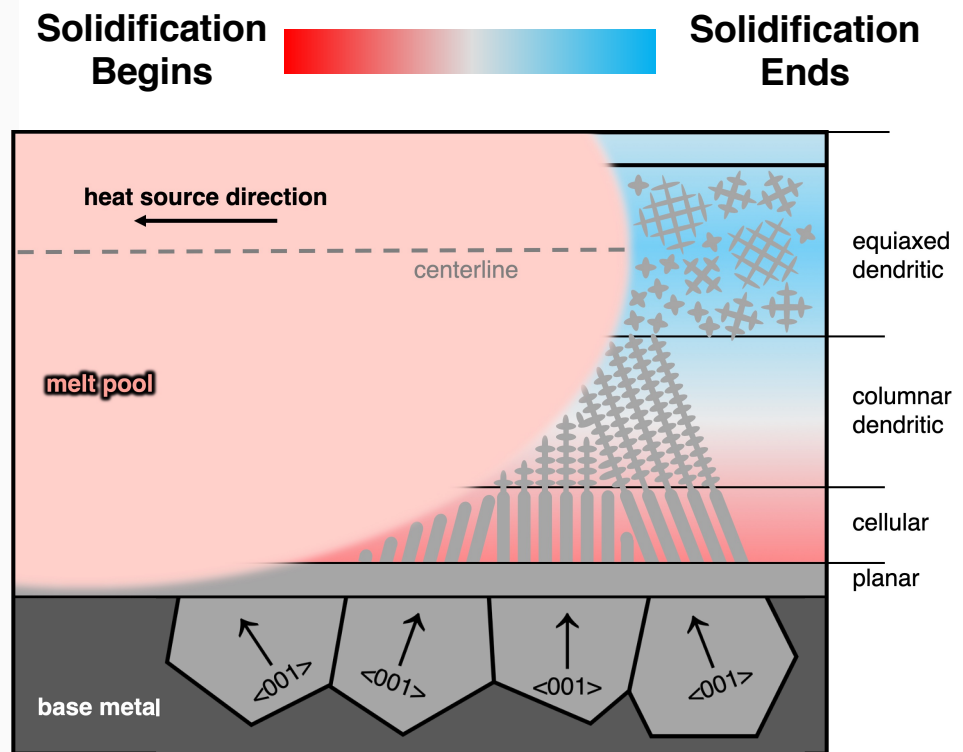
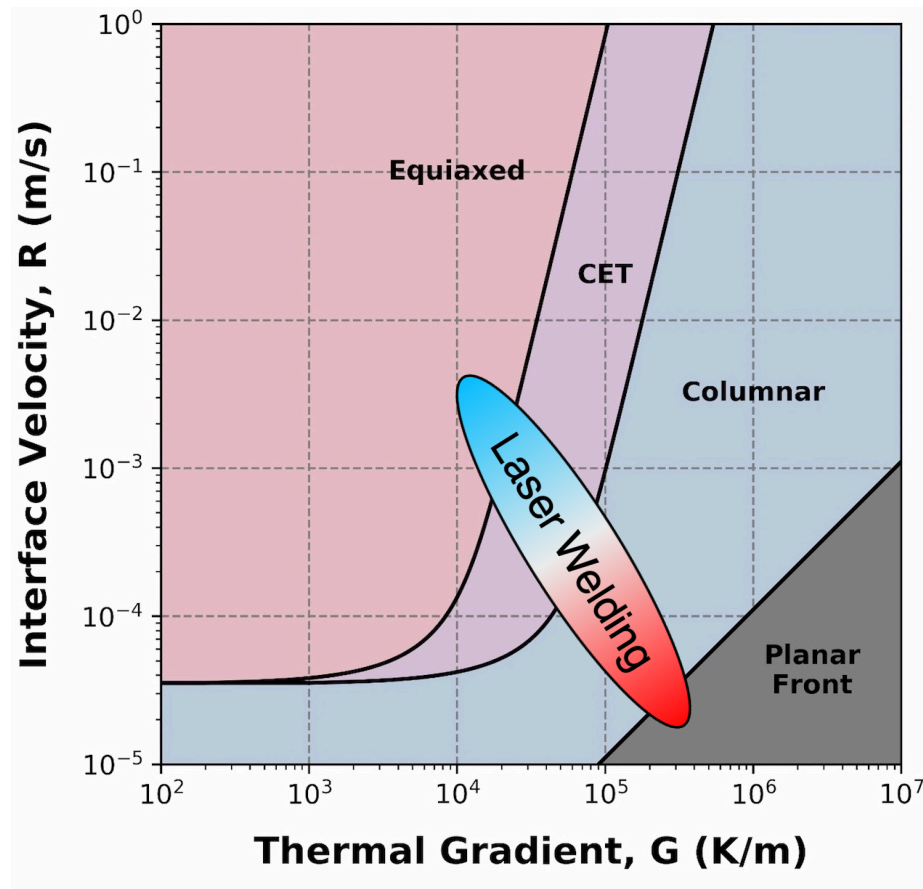
# Local microstructure control relies on understanding solidification conditions

- Solidification conditions are not static



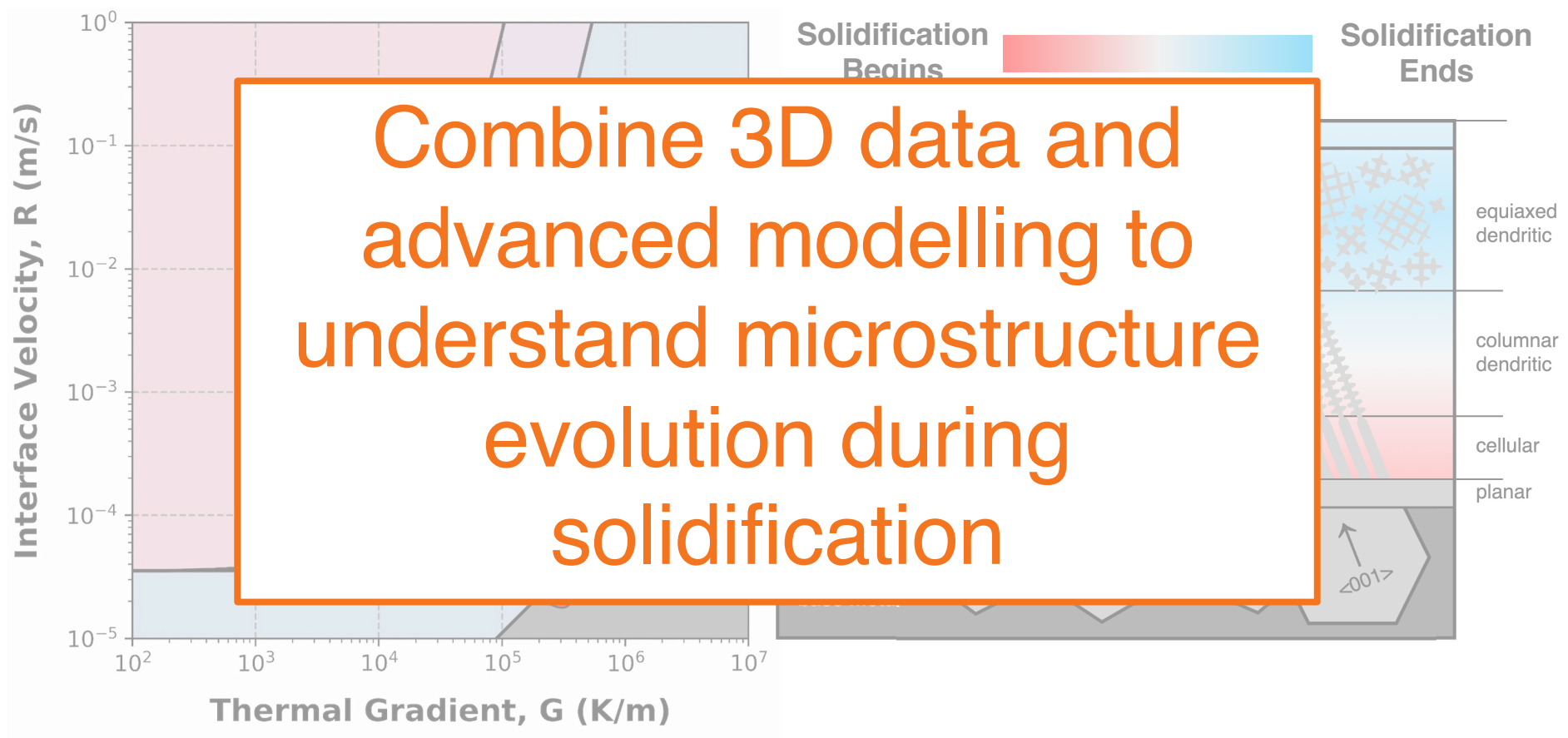
# Local microstructure control relies on understanding solidification conditions

- Solidification conditions are not static



# Local microstructure control relies on understanding solidification conditions

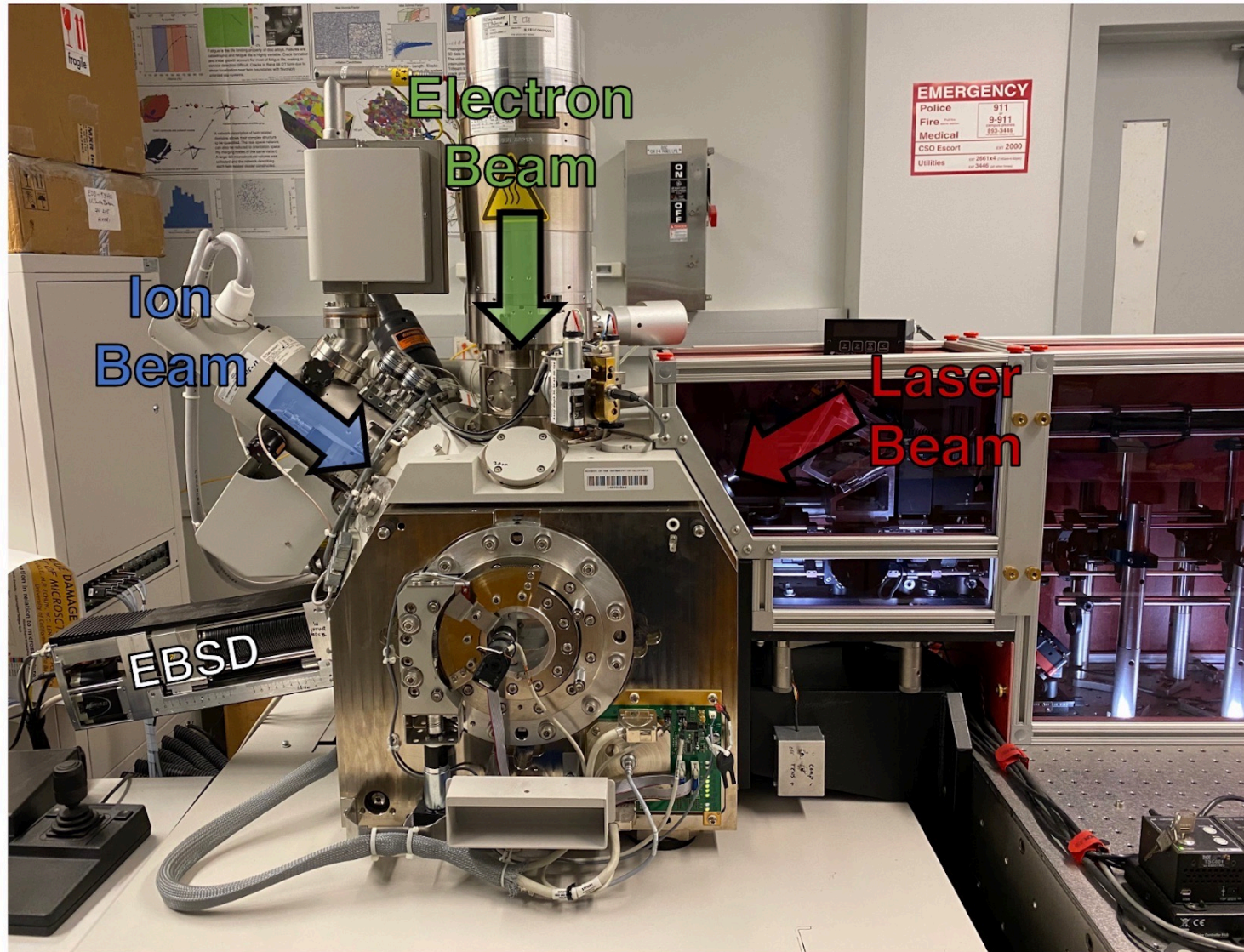
- Solidification conditions are not static



# Outline

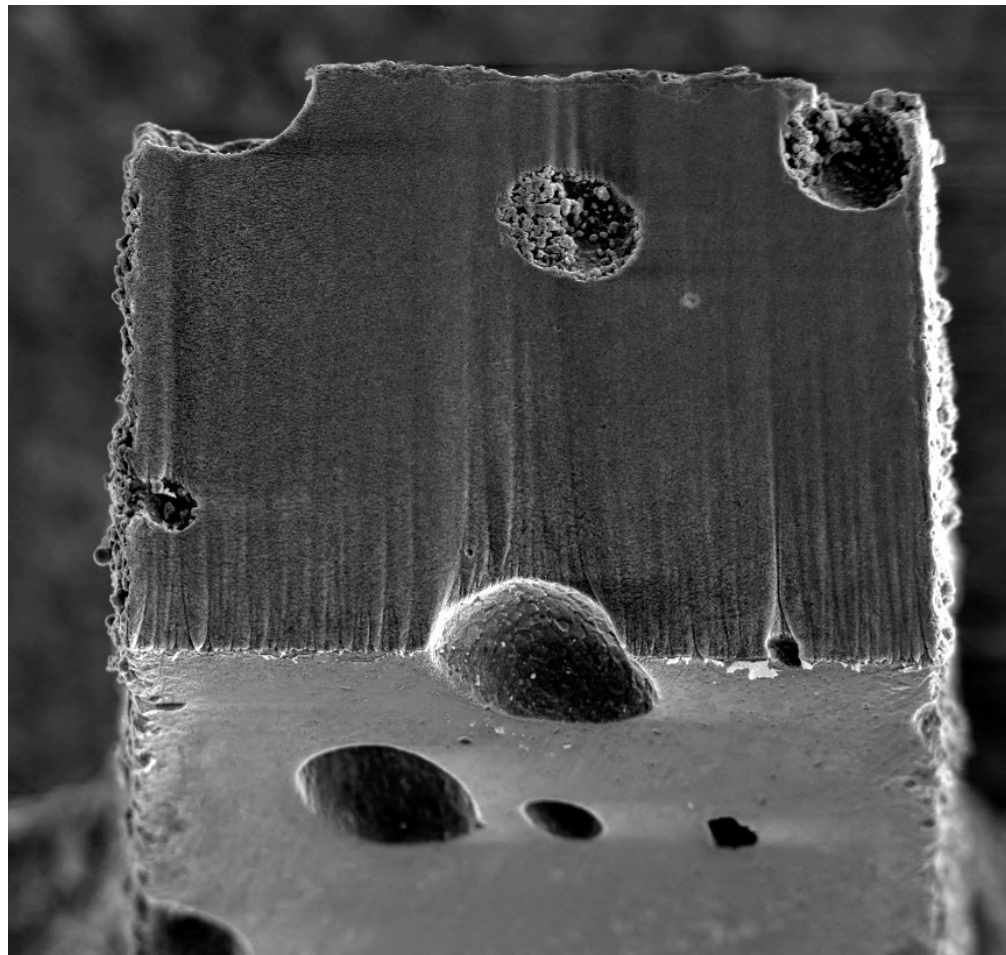
- Background
- Three-dimensional Characterization
- Calibrating a Microstructure-Processing Map
- Summary

# The TriBeam collects rich multi-modal datasets in three dimensions



# TriBeam tomography generates data in a set of slices

- Secondary electron images taken after laser machining\*

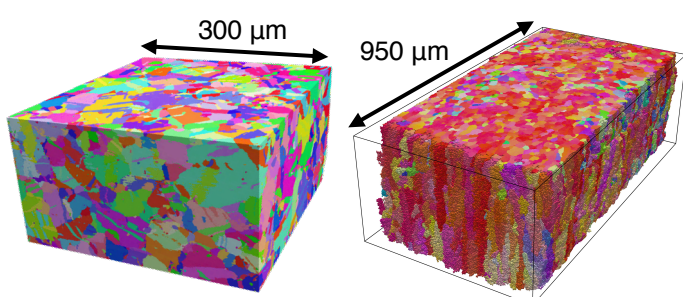


250  $\mu\text{m}$

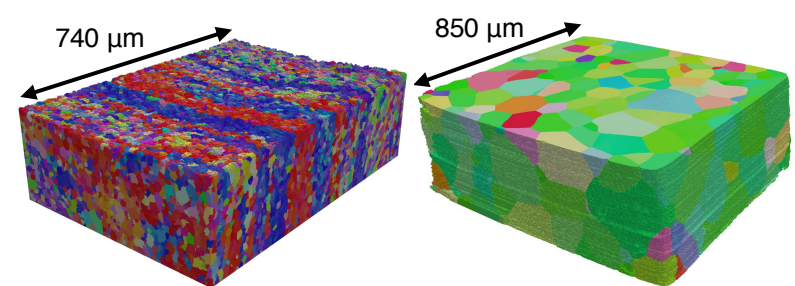
\*Additively Manufactured AlNiCo magnet

# Femtosecond laser ablation makes the TriBeam material agnostic

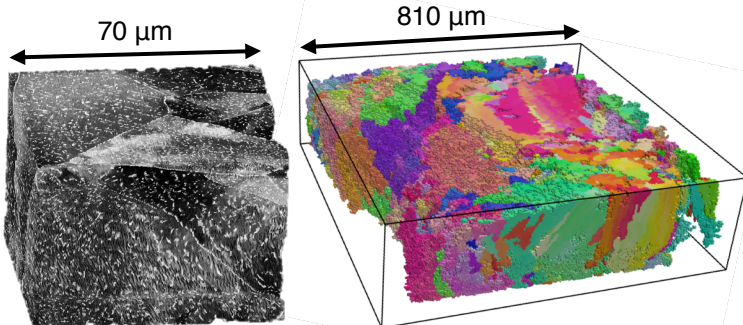
**Nickel Superalloys**



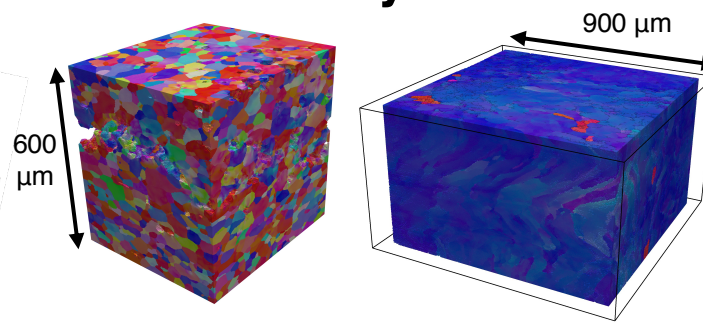
**Titanium Alloys**



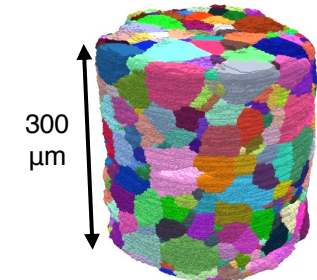
**Steels**



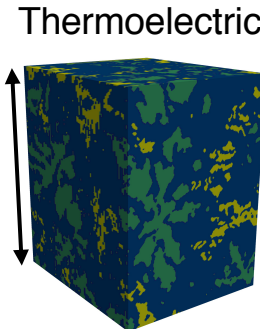
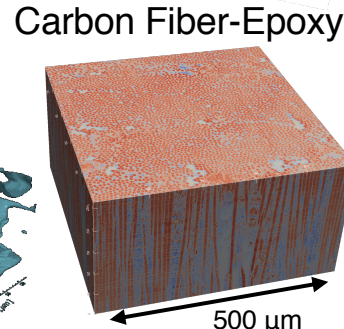
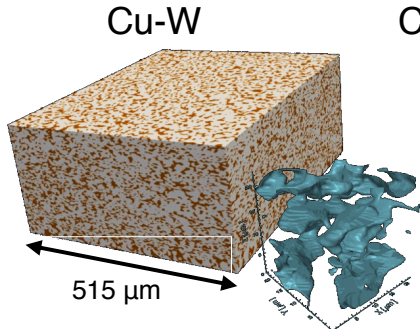
**Refractory Metals**



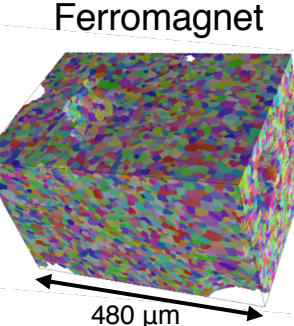
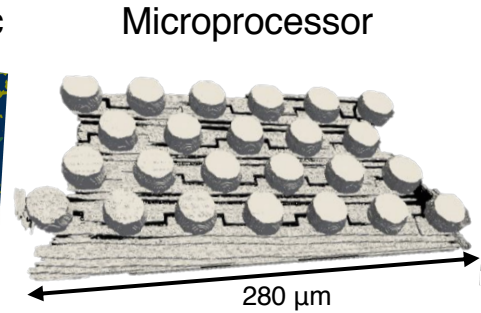
**Ceramics**



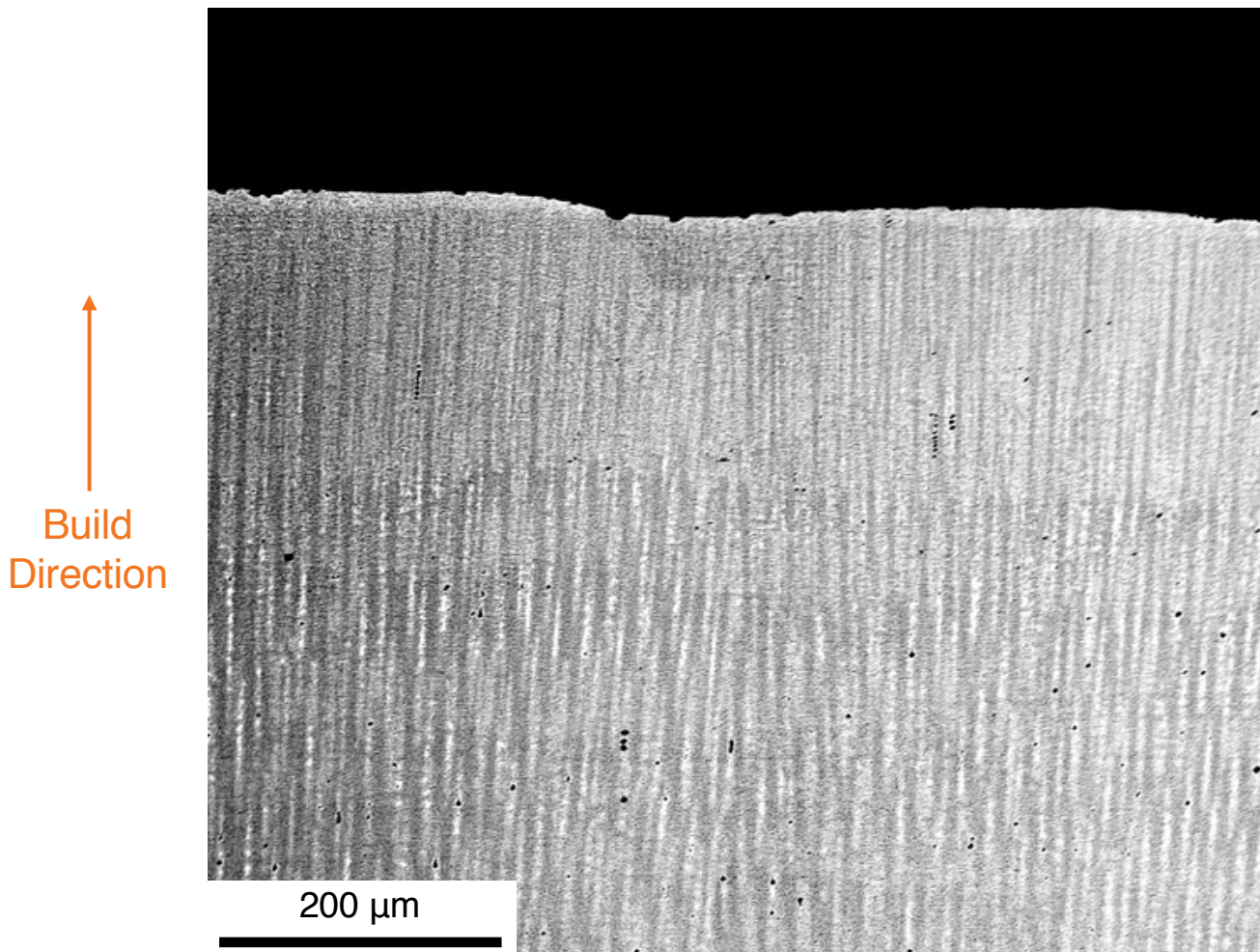
**Composites**



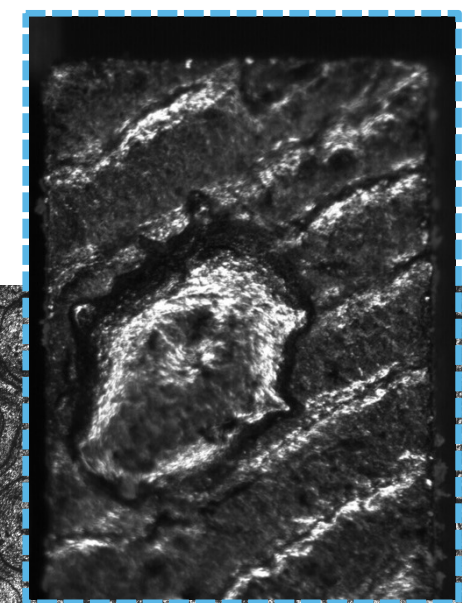
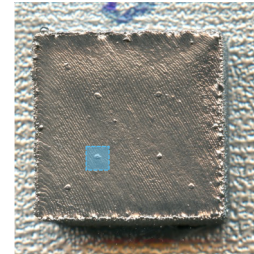
**Electronic Materials**



# Isolated melt pool on a bulk raster block



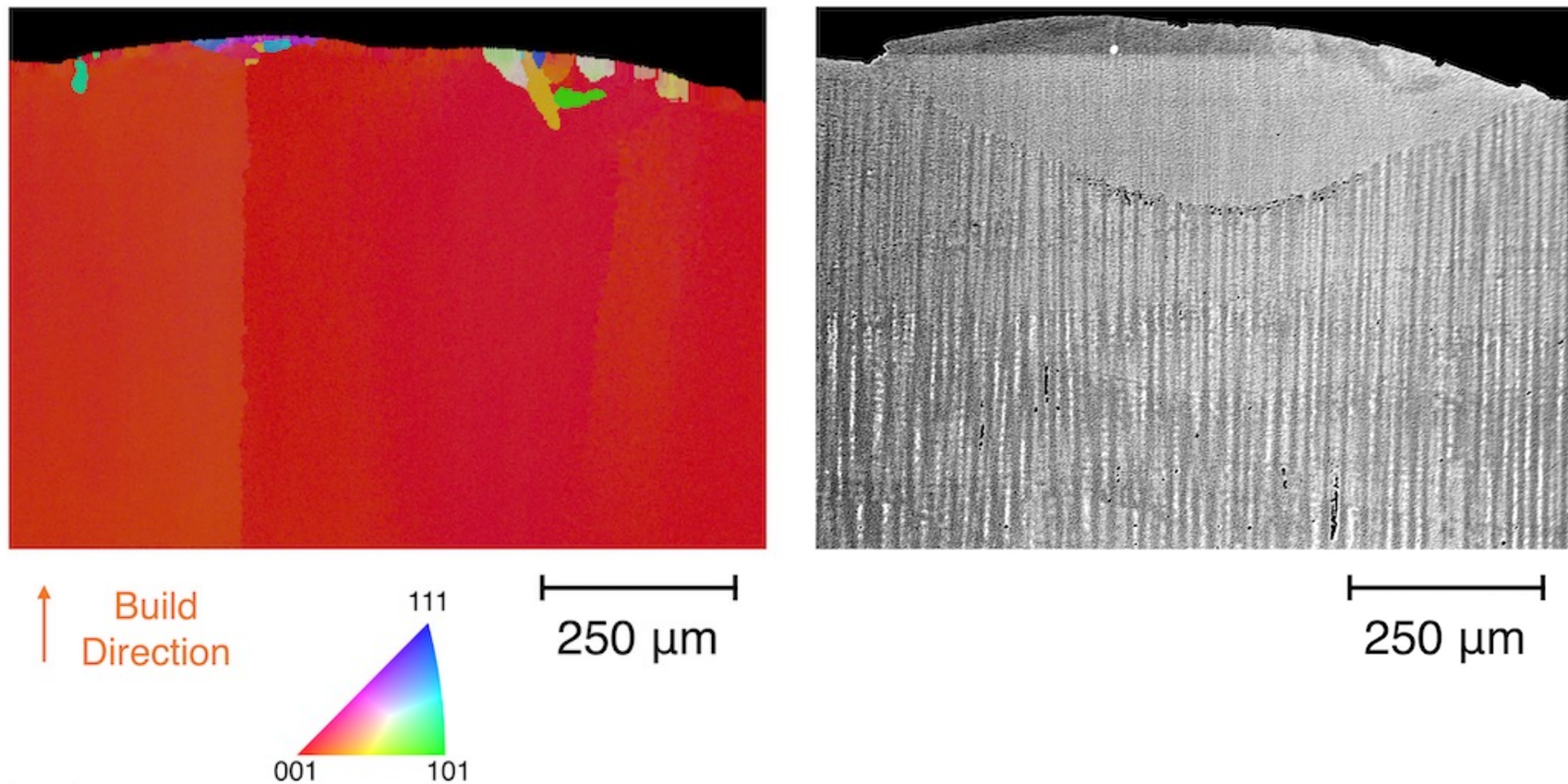
Raster Melt



Build Direction

# EBSD data shows nucleated grains, BSE data shows melt pool boundary

- Can fuse data modalities using TPS algorithm in 3D
- Also removes any distortions in EBSD data



# Data fusion can be achieved via the Thin Plate Spline Algorithm (TPS)\*

**Distorted frame is a function of the reference frame**

$$(X, Y, Z) = f(x, y, z)$$

$$(X, Y, Z) = f(x, y, z) = a_1 + a_x x + a_y y + a_z z + \sum_{i=1}^n w_i U(|P_i - (x, y, z)|)$$

Affine Portion Bending Portion

- Radial basis function:

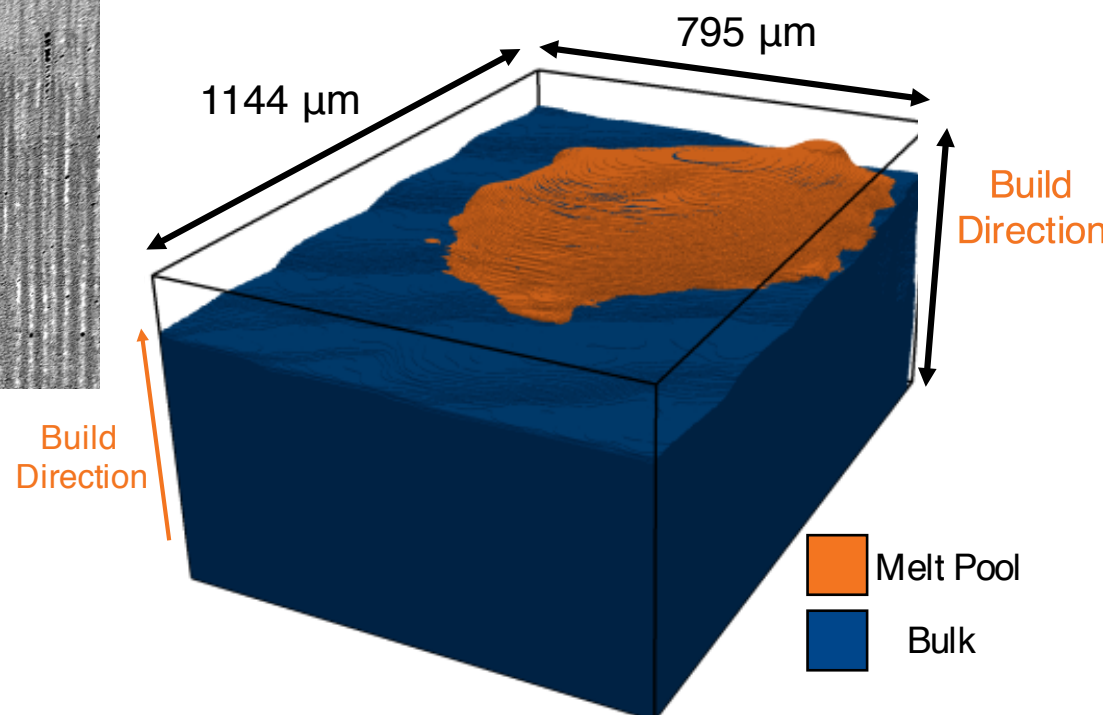
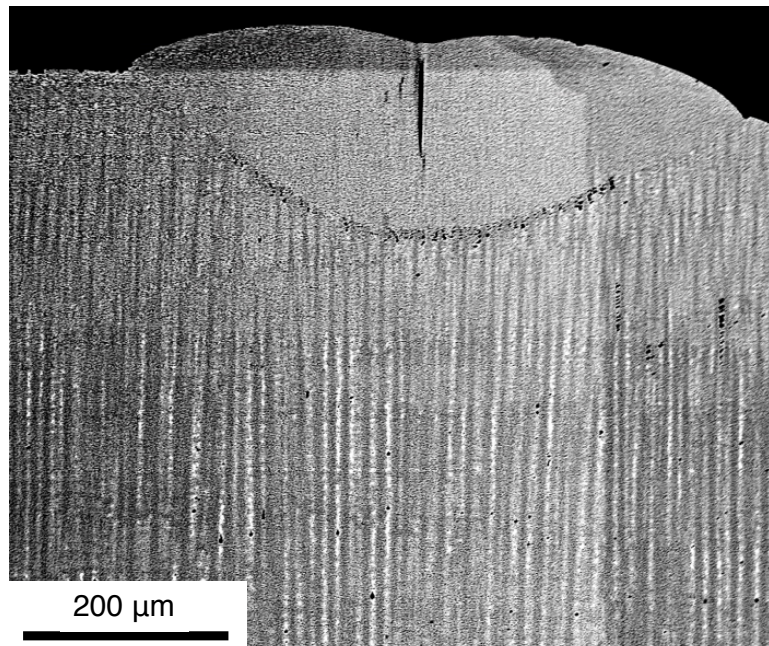
$$U(r) = r^2 \log(r^2)$$

- Solve for weighting coefficients  $w_i$  and  $a_1, a_x, a_y$ , and  $a_z$  using  $n$  control points (CP) to create a system of  $n+4$  equations
  - CPs are shared locations in distorted  $(X_i, Y_i, Z_i)$  and reference  $(x_i, y_i, z_i)$  images
    - Triple points, voids, precipitates, sample edges

\*Extended to 3D using 2D form described in Y. B. Zhang, A Elbrond, F. X. Lin, *Materials Characterization* (2014)

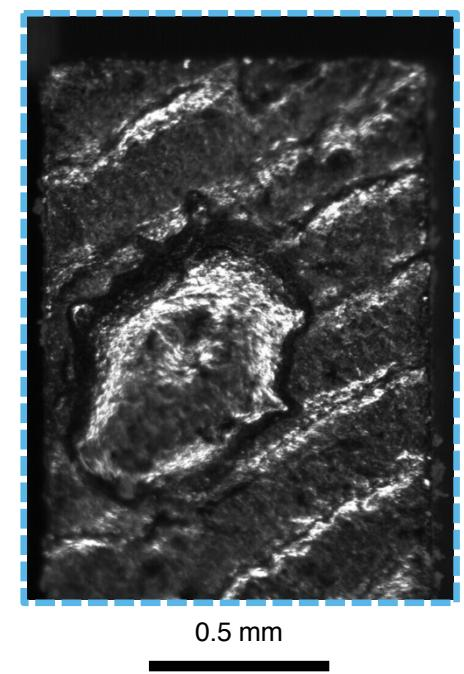
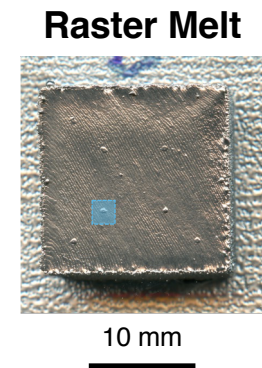
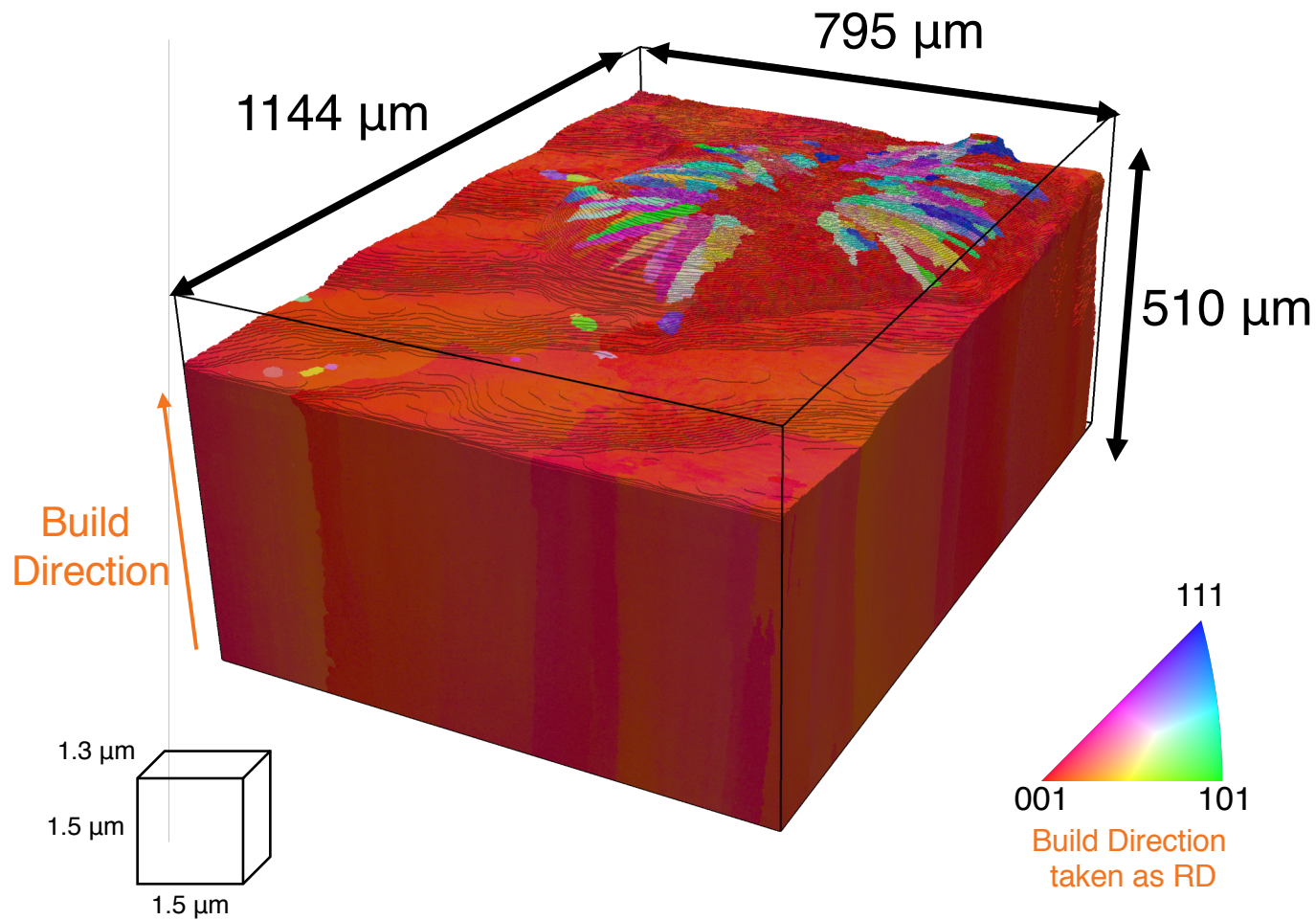
# EBSD aligned with BS imaging using TPS, allowing melt pool segmentation

- 3894 control points used for thin plate spline algorithm



# Reconstruction of isolated melt pool on a bulk raster block

- 878 slices collected (~20 minutes per slice)
  - 3.6 TB of data



Build Direction

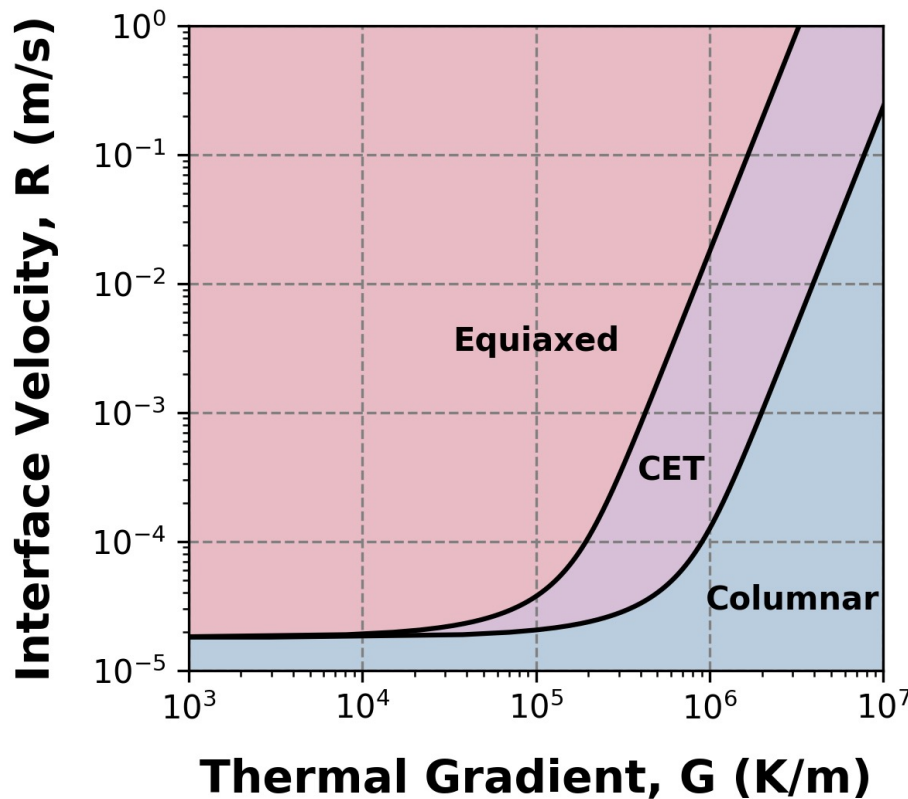
22

# Outline

- Background
- Three-dimensional Characterization
- Calibrating a Microstructure-Processing Map
- Summary

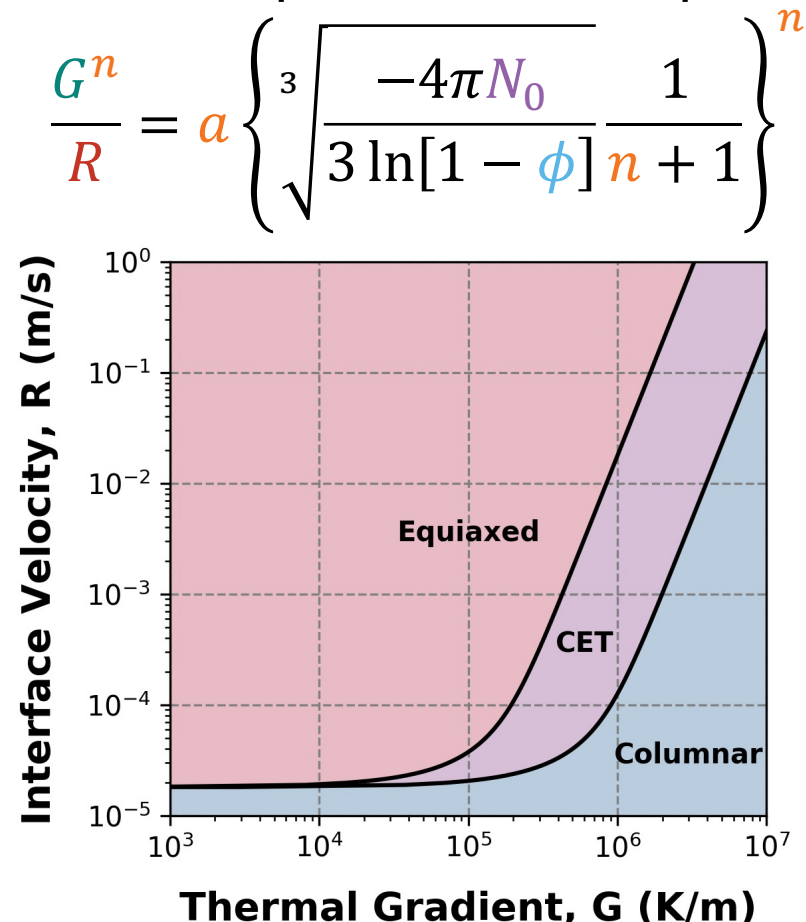
# Need to accurately predict the columnar to equiaxed transition (CET)

$$G = \frac{1}{n+1} \sqrt[3]{\frac{-4\pi N_0}{3 \ln [1 - \phi]}} \cdot \left( 1 - \frac{\Delta T_n^{n+1}}{(a \cdot R)^{(n+1)/n}} \right) \cdot (a \cdot R)^{1/n}$$



# Need to accurately predict the columnar to equiaxed transition (CET)

- Gäumann's modification of Hunt's CET model at high G
  - Developed for laser deposition on single-crystal Ni superalloys



$G$  = Thermal Gradient

$R$  = Interface Velocity

$N_0$  = Nuclei density

$a, n$  = Material constants

$\phi$  = Probability of  
grain nucleation  
ahead of interface

# Need to accurately predict the columnar to equiaxed transition (CET)

- Gäumann's modification of Hunt's CET model at high G
  - Developed for laser deposition on single-crystal Ni superalloys

$$\frac{G^n}{R} = \alpha \left\{ \sqrt[3]{\frac{-4\pi N_0}{3 \ln[1 - \phi]}} \frac{1}{n + 1} \right\}^n$$

Rearrange to yield:

$$\phi = 1 - \exp \left\{ \frac{-4\pi N_0 \alpha^{3/n}}{3(n+1)^3} \left( \frac{R}{G^n} \right)^{3/n} \right\}$$

$G$  = Thermal Gradient

$R$  = Interface Velocity

$N_0$  = Nuclei density

$\alpha, n$  = Material constants

$\phi$  = Probability of  
grain nucleation  
ahead of interface

# Checklist for Columnar to Equiaxed Transition (CET) Model

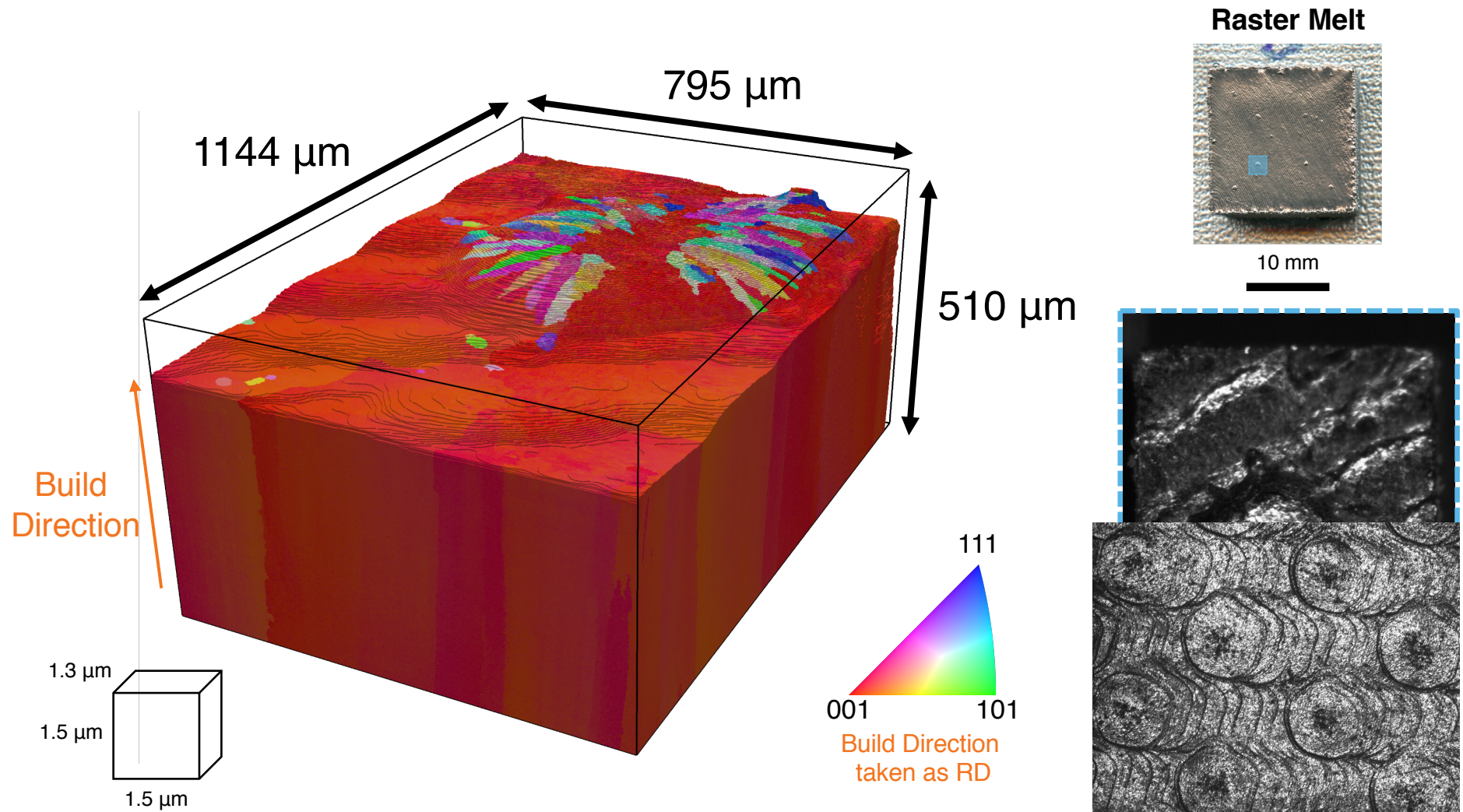
- Want to predict the formation of nucleated grains

$$\phi = 1 - \exp \left\{ \frac{-4\pi N_0 a^{3/n}}{3(n+1)^3} \left( \frac{R}{G^n} \right)^{3/n} \right\}$$

- $G$  = Thermal Gradient
- $R$  = Interface Velocity
- $N_0$  = Nuclei density
- $a, n$  = Material constants

$\phi$  = Probability of  
grain nucleation  
ahead of interface

# Apply model to isolated melt pool on top of raster melt block



# G and R can be calculated for this solidification event using TRUCHAS

- Want to predict the formation of nucleated grains

$$\phi = 1 - \exp \left\{ \frac{-4\pi N_0 a^{3/n}}{3(n+1)^3} \left( \frac{R}{G^n} \right)^{3/n} \right\}$$

TRUCHAS

$\phi$  = Probability of grain nucleation ahead of interface

$G$  = Thermal Gradient

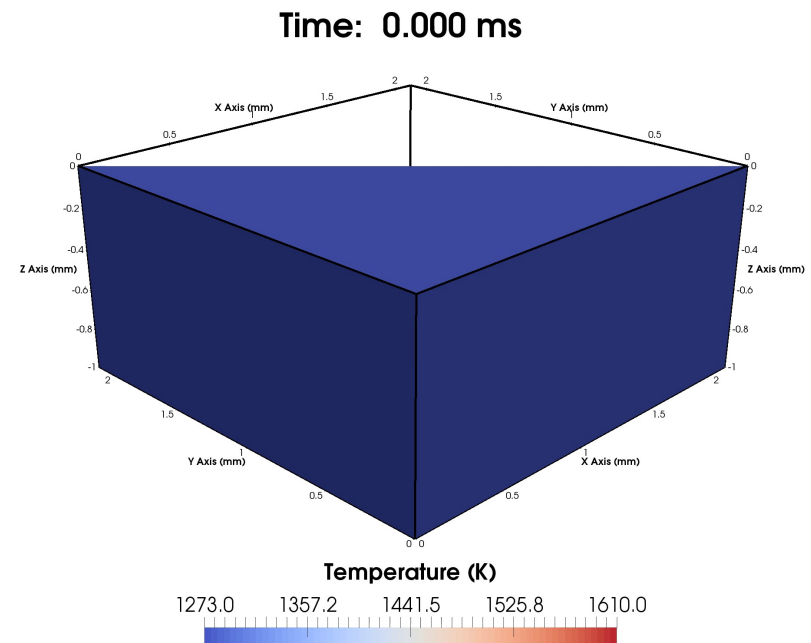
$R$  = Interface Velocity

$N_0$  = Nuclei density

$a, n$  = Material constants

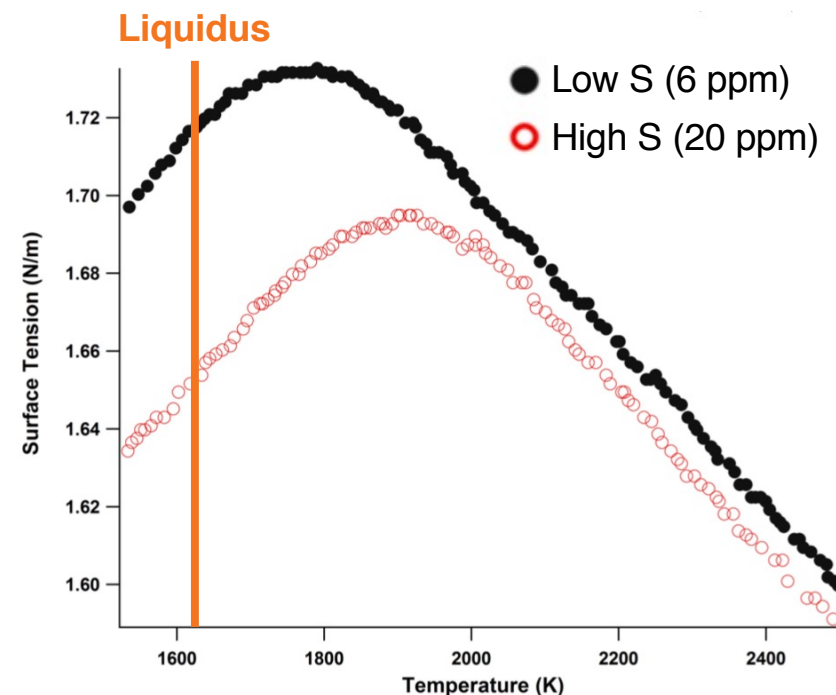
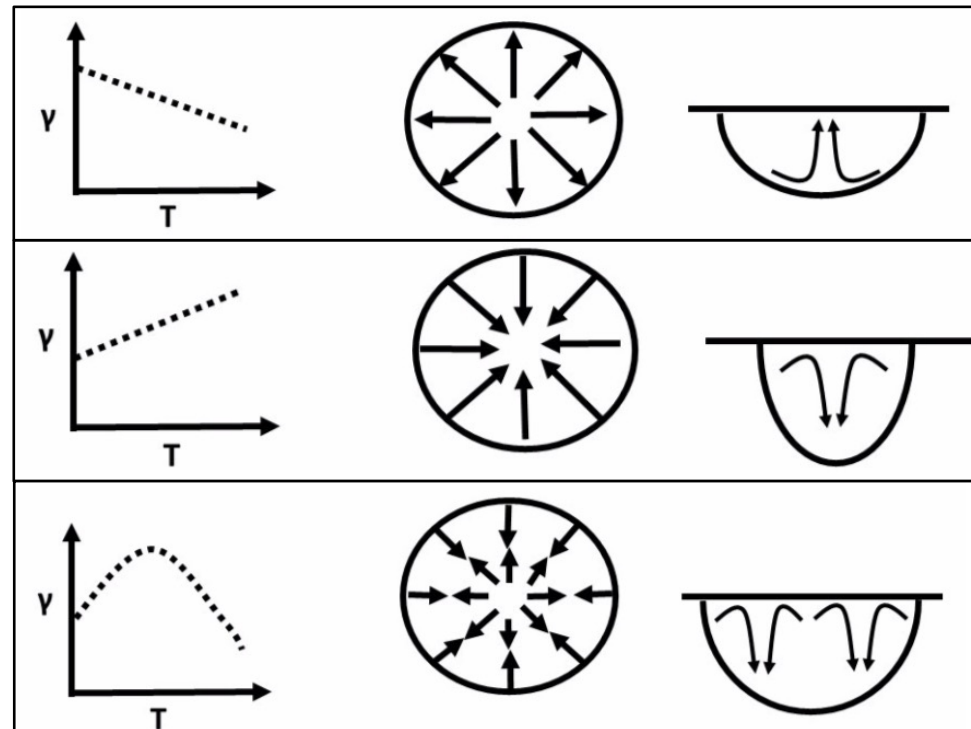
# Can use TRUCHAS to model differences in temperature profile during solidification

- Can model heat transfer and fluid flow
  - Designed for casting, so does not currently consider powder-beam interactions or multiple melt layers
- Enables 3D calculation of thermal gradient and solid-liquid interface velocity on  $\mu\text{m}$  and  $\text{ms}$  scales
  - Inaccessible to in-situ monitoring
- Code has been validated against Abaqus and that of Debroy et al.



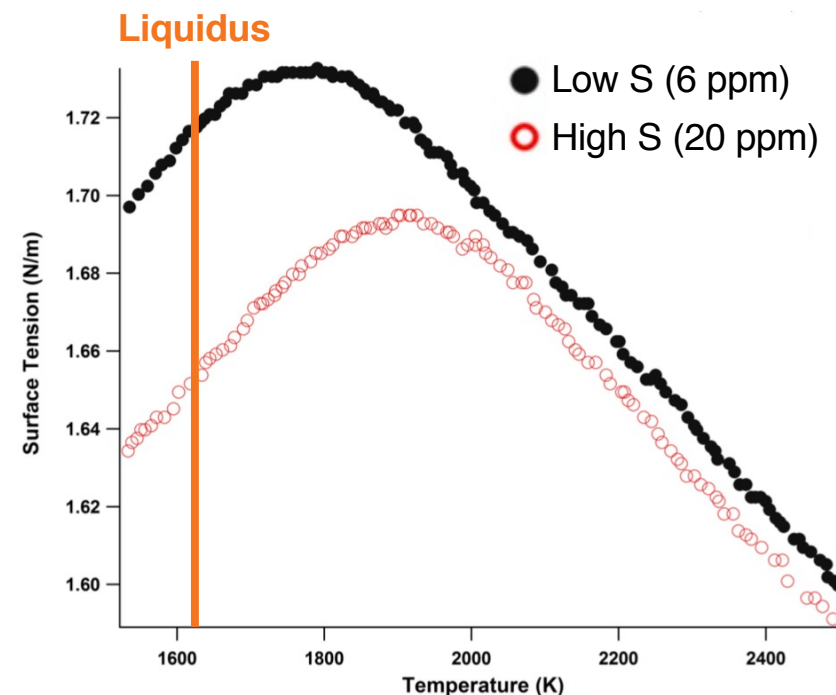
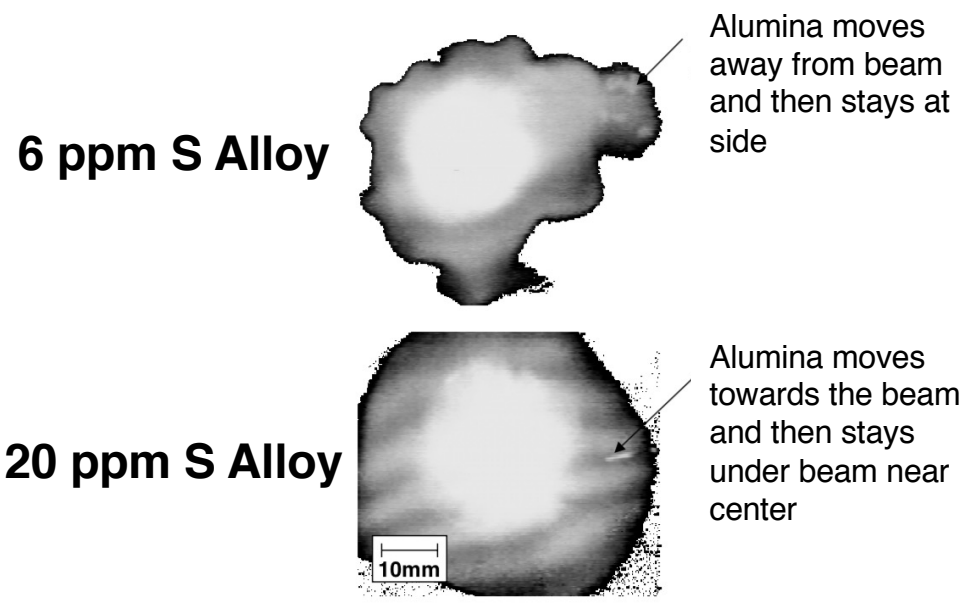
# TRUCHAS Simulations performed with and without fluid flow

- Performed simulations with relevant beam settings
  - 10 mA 0.5 ms dwell, 1273 K preheat
  - All simulations with heat transfer, two also include fluid flow
    - Fluid flow incorporates temperature dependence of surface tension ( $\gamma$ )



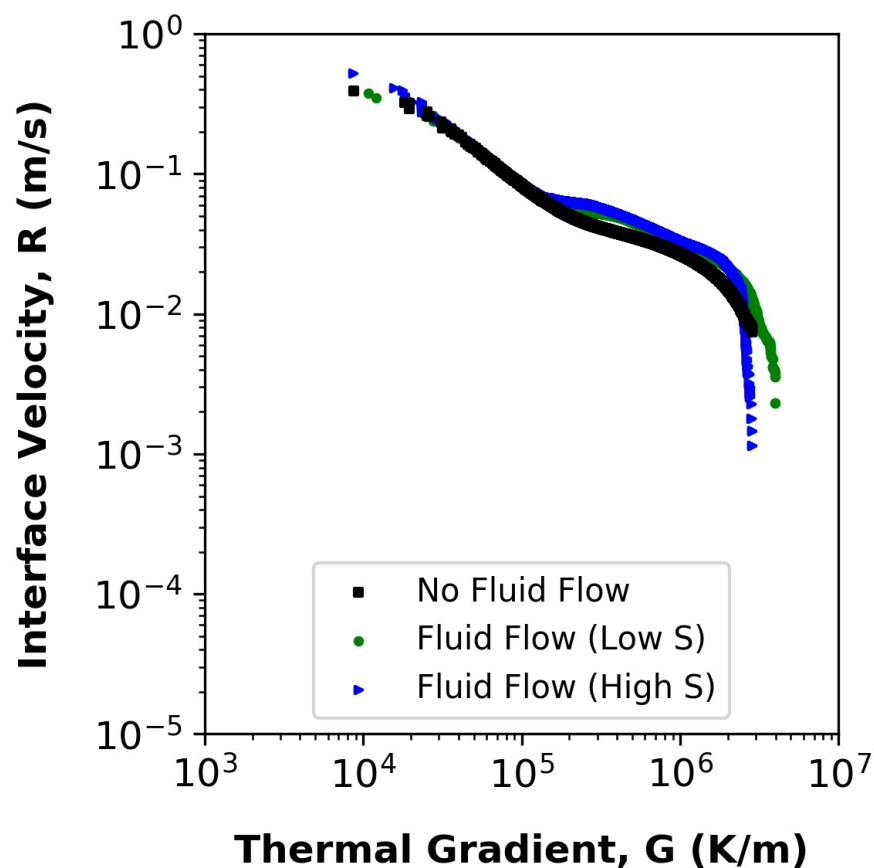
# TRUCHAS Simulations performed with and without fluid flow

- Performed simulations with relevant beam settings
  - 10 mA 0.5 ms dwell, 1273 K preheat
  - All simulations with heat transfer, two also include fluid flow
    - Fluid flow incorporates temperature dependence of surface tension ( $\gamma$ )



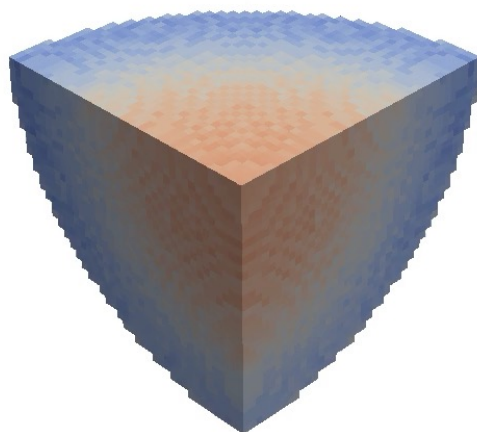
# Results of TRUCHAS simulations

- Incorporation of fluid flow increases interface velocity in middle stages of solidification

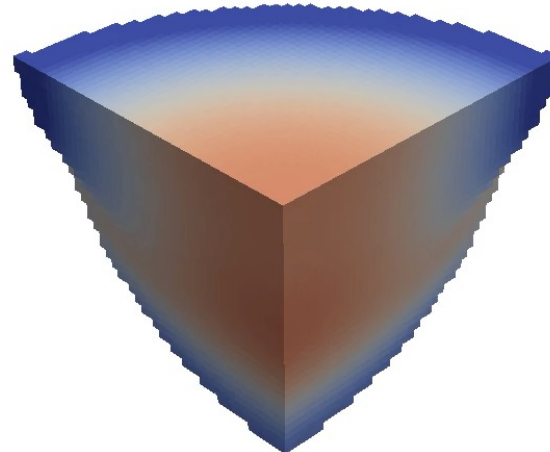


# Higher S content increases local solidification time

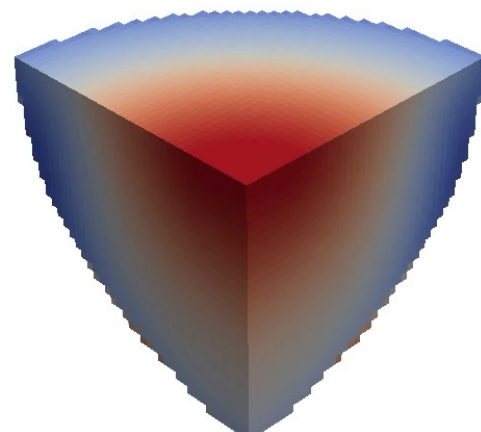
**No Fluid Flow**



**Fluid Flow (Low S)**



**Fluid Flow (High S)**

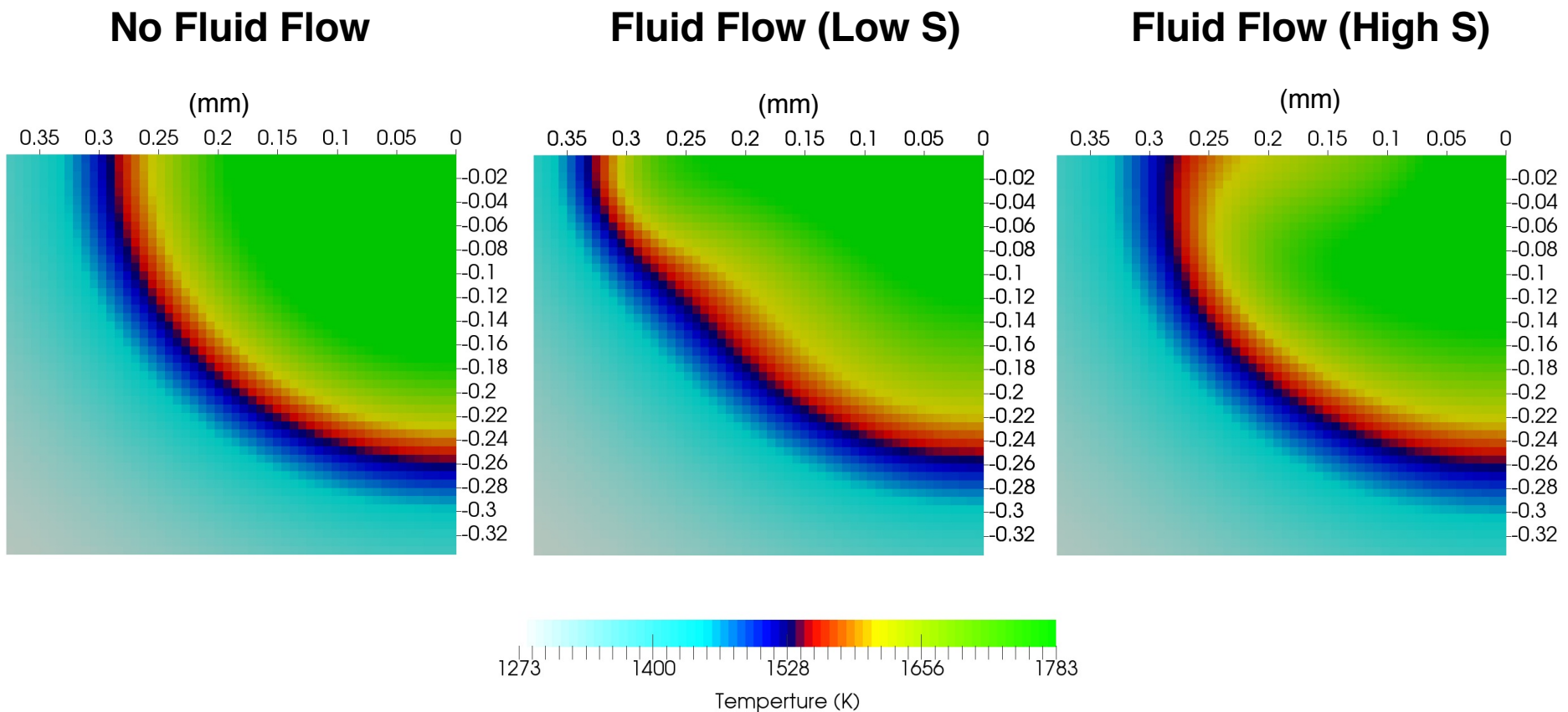


**Local Solidification Time (ms)**



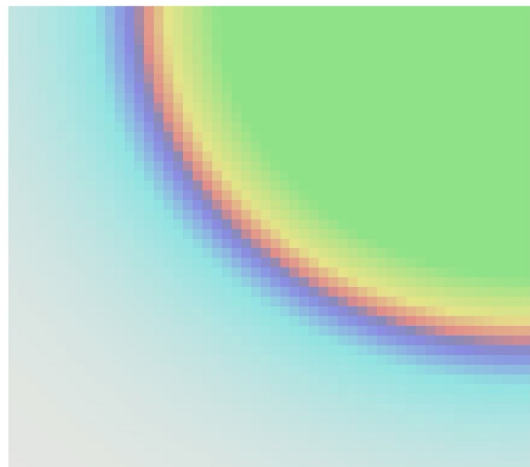
# Pool spreads more with lower S content, which is also seen in 304 steel welds

- Fully Solid, Mushy Zone, and Fully Liquid
- Maximum extent of melt pool at  $t \approx 3$  ms



# Visualizing fluid flow

Time: 2.014583



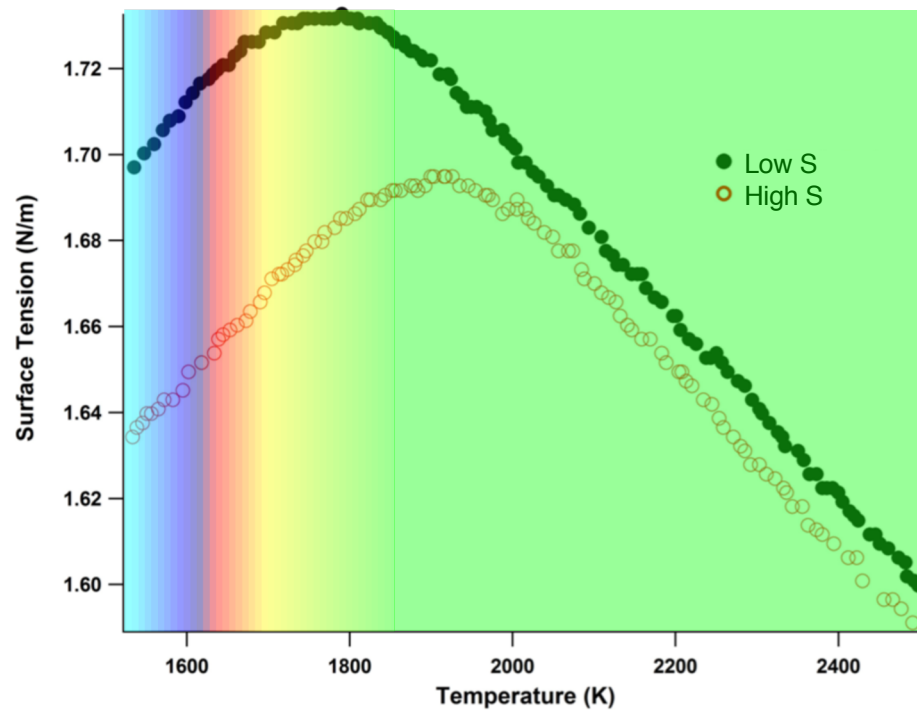
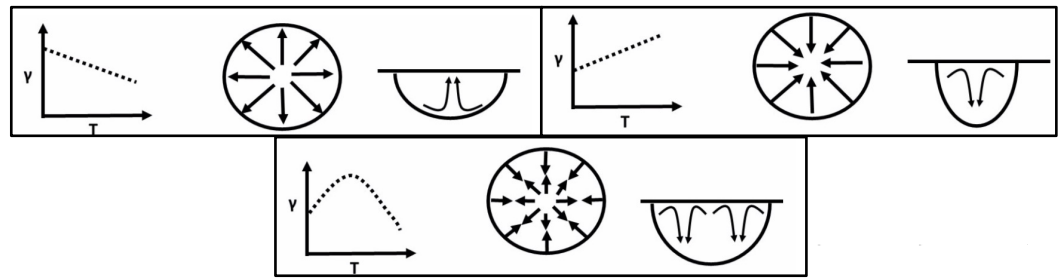
Low S  
Fluid  
Flow

Time: 2.014583



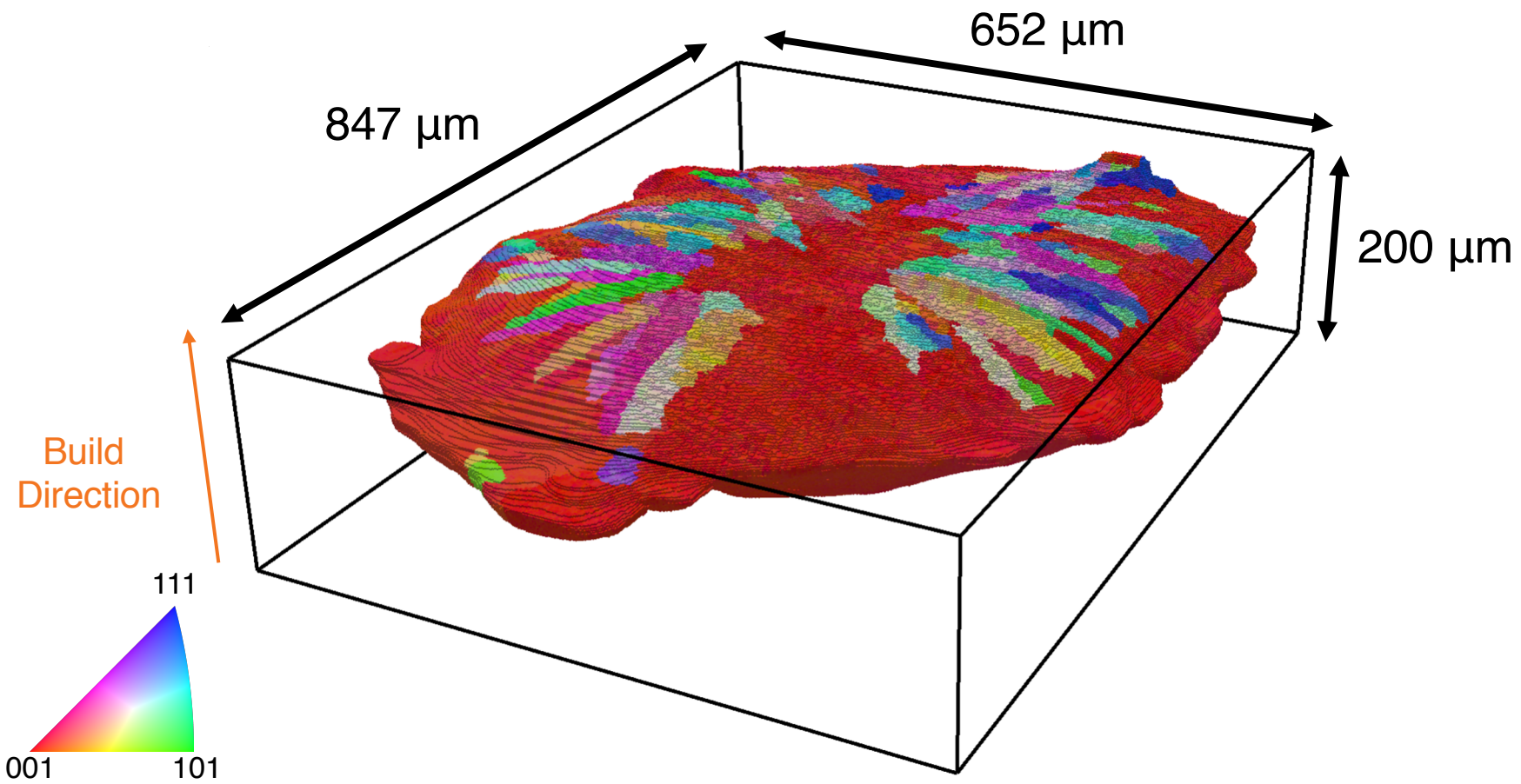
High S  
Fluid  
Flow

1273 1400 1528 1656 1783  
Temperture (K)



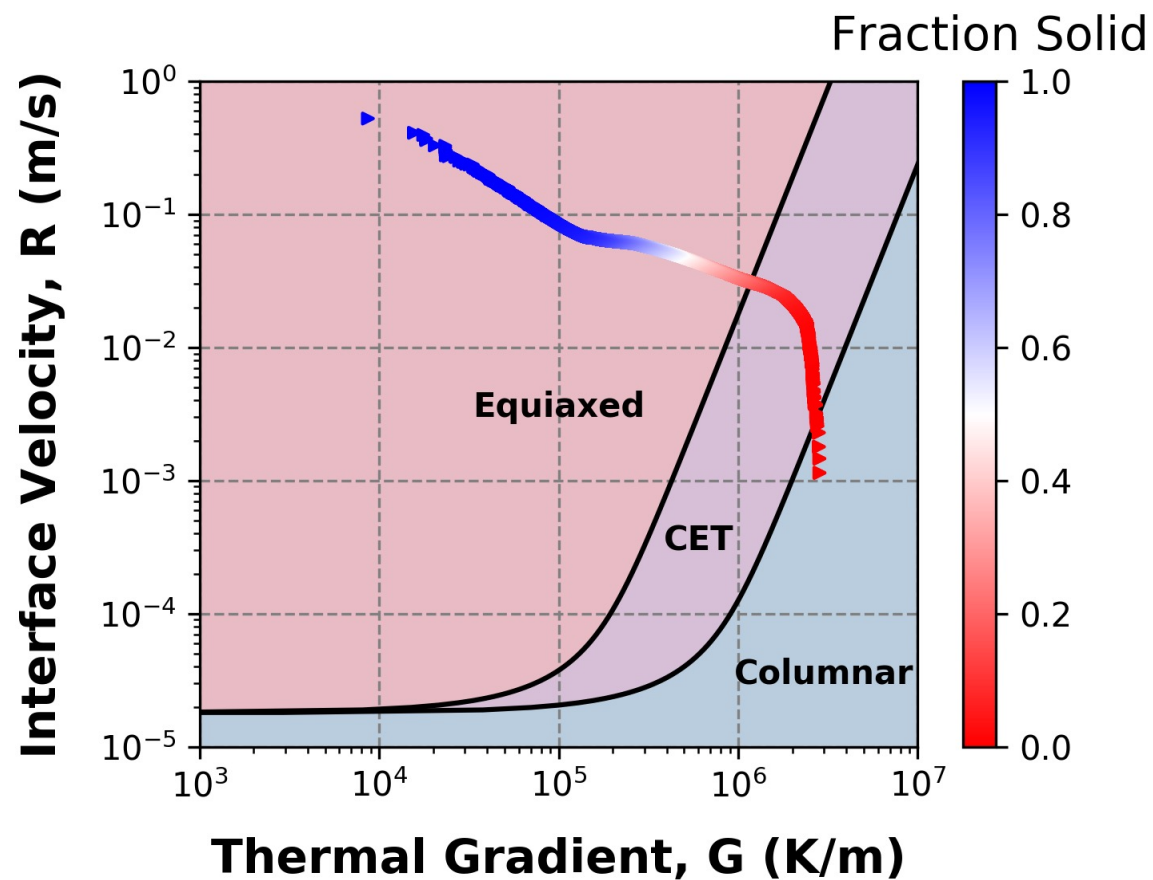
# Isolated melt pool from full dataset

- Nucleated grains form radially around center of pool



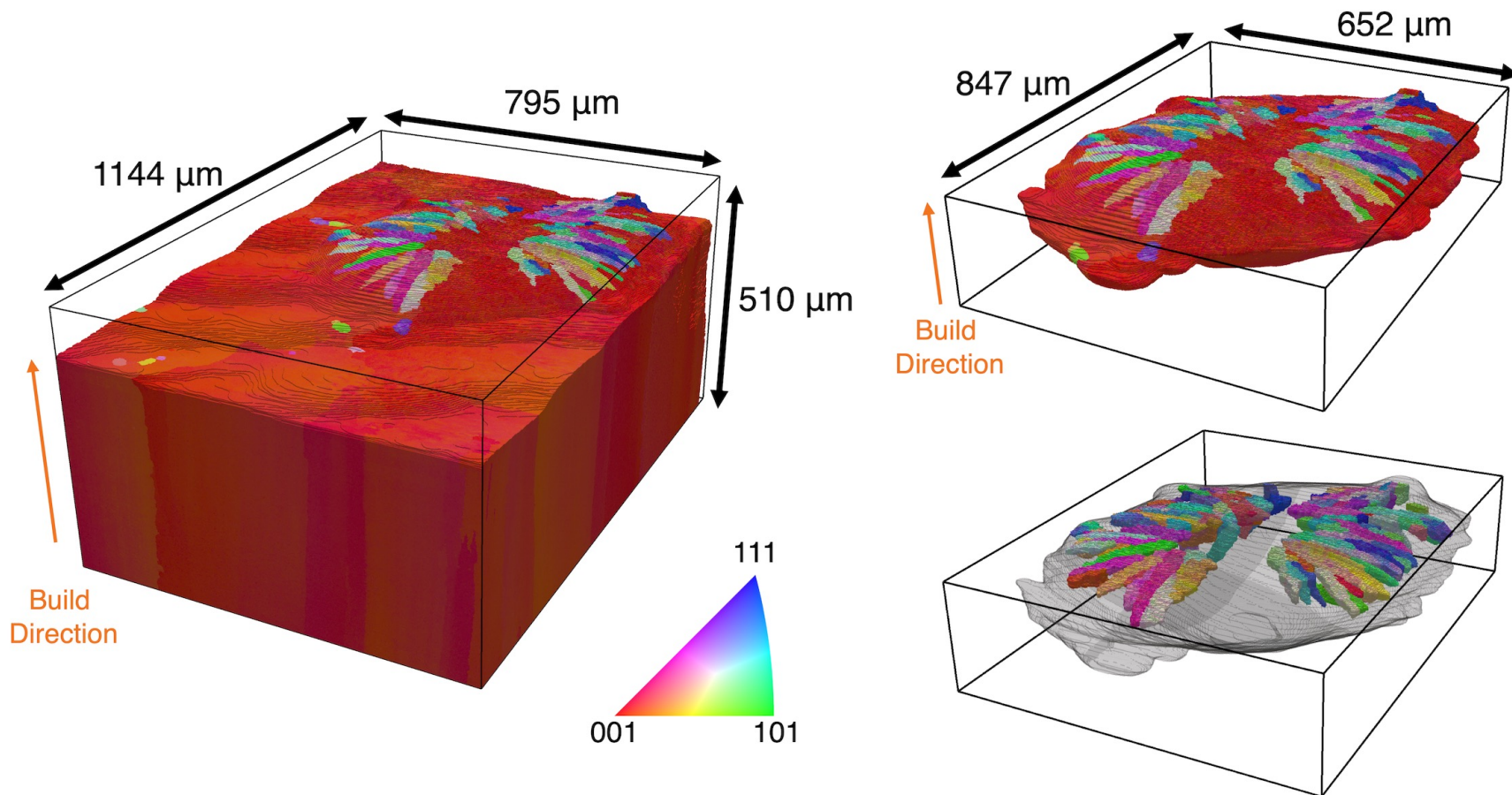
# Results of TRUCHAS simulations

- Predicts nucleated grain fraction ( $\Phi$ ) of **80.8%**



# Results of TRUCHAS simulations

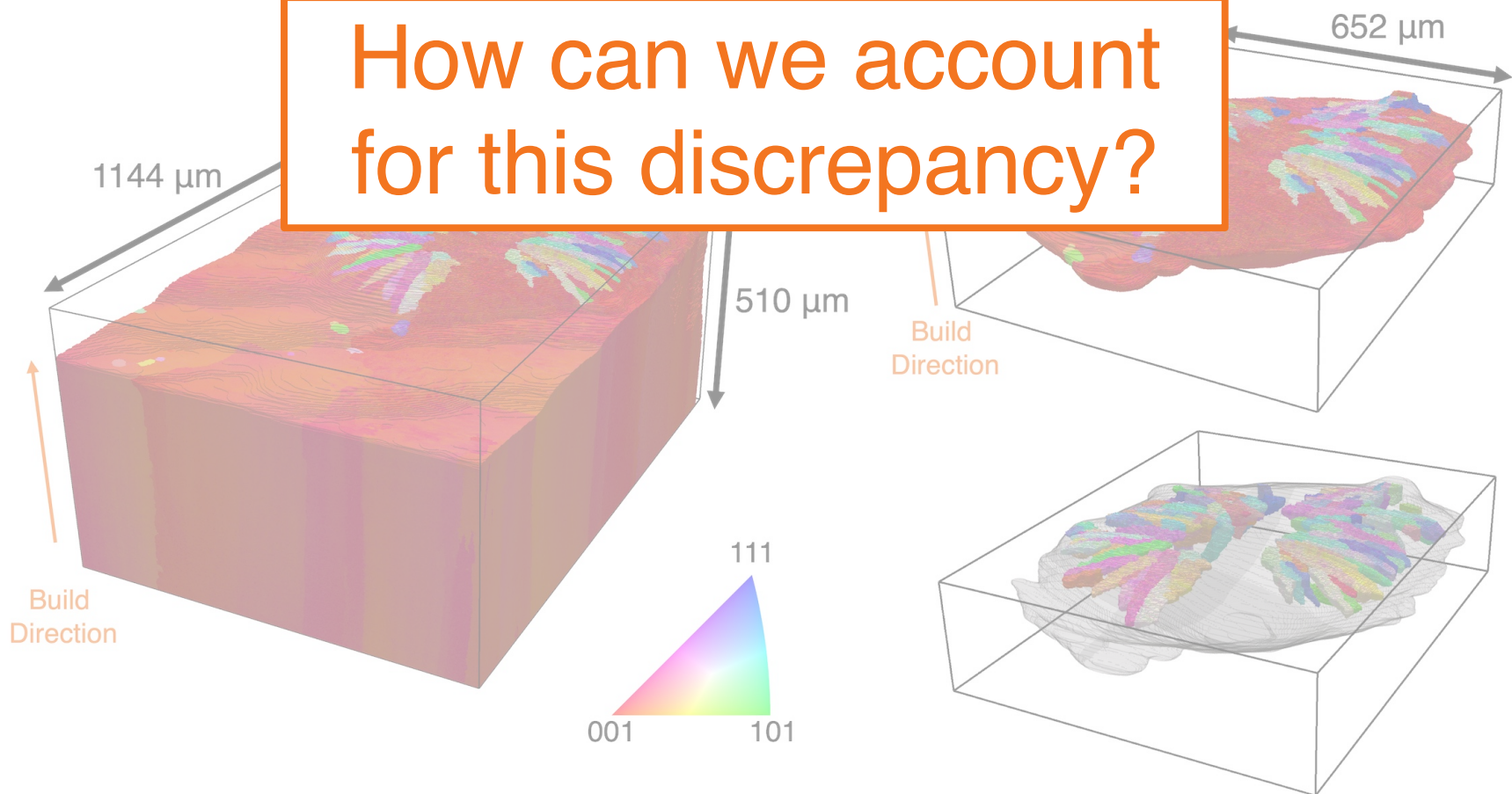
- Predicted nucleated grain fraction ( $\Phi$ ) of **80.8%**
- Measured nucleated grain fraction ( $\Phi$ ) of **11.4%**



# Results of TRUCHAS simulations

- Predicted nucleated grain fraction ( $\Phi$ ) of **80.8%**
- Measured nucleated grain fraction ( $\Phi$ ) of **11.4%**

How can we account  
for this discrepancy?



# Checklist for Columnar to Equiaxed Transition (CET) Model

- Want to predict the formation of nucleated grains

$$\phi = 1 - \exp \left\{ \frac{-4\pi N_0 a^{3/n}}{3(n+1)^3} \left( \frac{R}{G^n} \right)^{3/n} \right\}$$

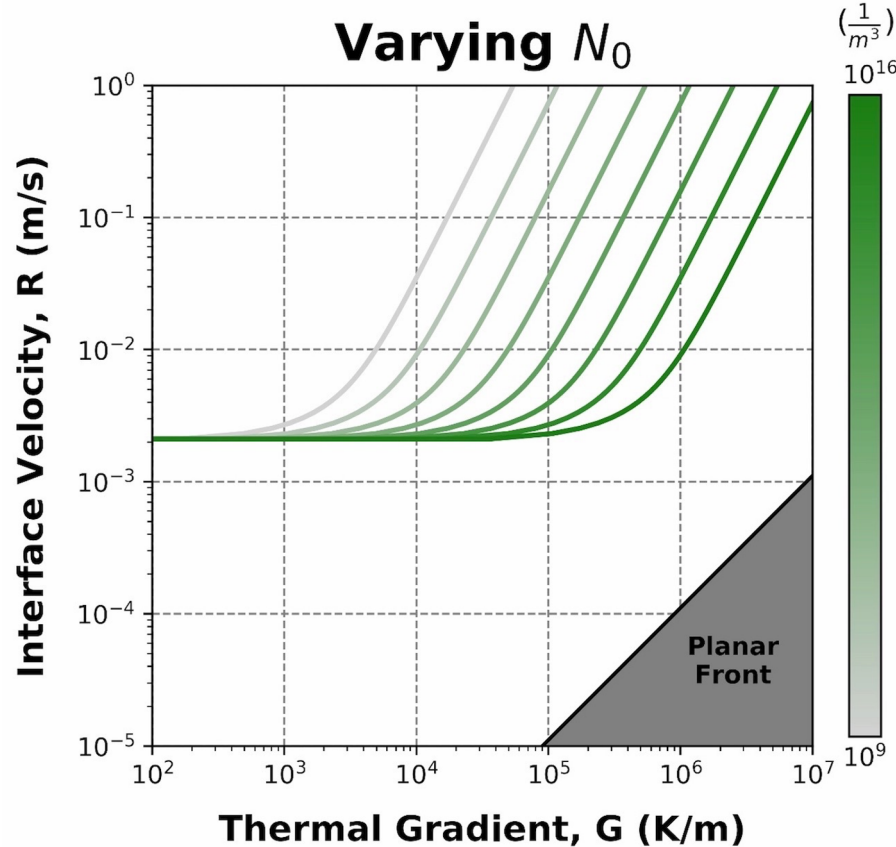
TRUCHAS

<input checked="" type="checkbox"/>	$G$ = Thermal Gradient
<input checked="" type="checkbox"/>	$R$ = Interface Velocity
<input type="checkbox"/>	$N_0$ = Nuclei density
<input type="checkbox"/>	$a, n$ = Material constants
$\phi$ = Probability of grain nucleation ahead of interface	

# Checklist for Columnar to Equiaxed Transition (CET) Model

- Want to predict the formation of nucleated grains

$$\phi = 1 - \exp \left\{ \frac{-4\pi N_0 a^{3/n}}{3(n+1)^3} \left( \frac{R}{G^n} \right)^{3/n} \right\}$$

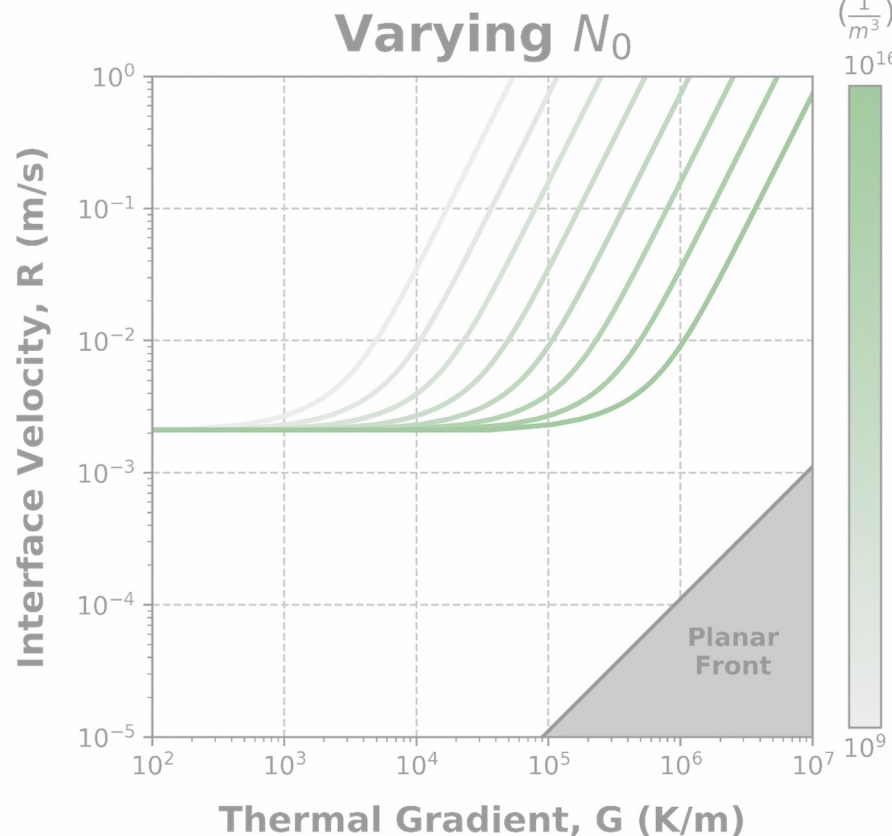


- $G$  = Thermal Gradient
- $R$  = Interface Velocity
- $N_0$  = Nuclei density
- $a, n$  = Material constants
- $\phi$  = Probability of grain nucleation ahead of interface

# Checklist for Columnar to Equiaxed Transition (CET) Model

- Want to predict the formation of nucleated grains

$$\phi = 1 - \exp \left\{ \frac{-4\pi N_0 a^{3/n}}{3(n+1)^3} \left( \frac{R}{G^n} \right)^{3/n} \right\}$$



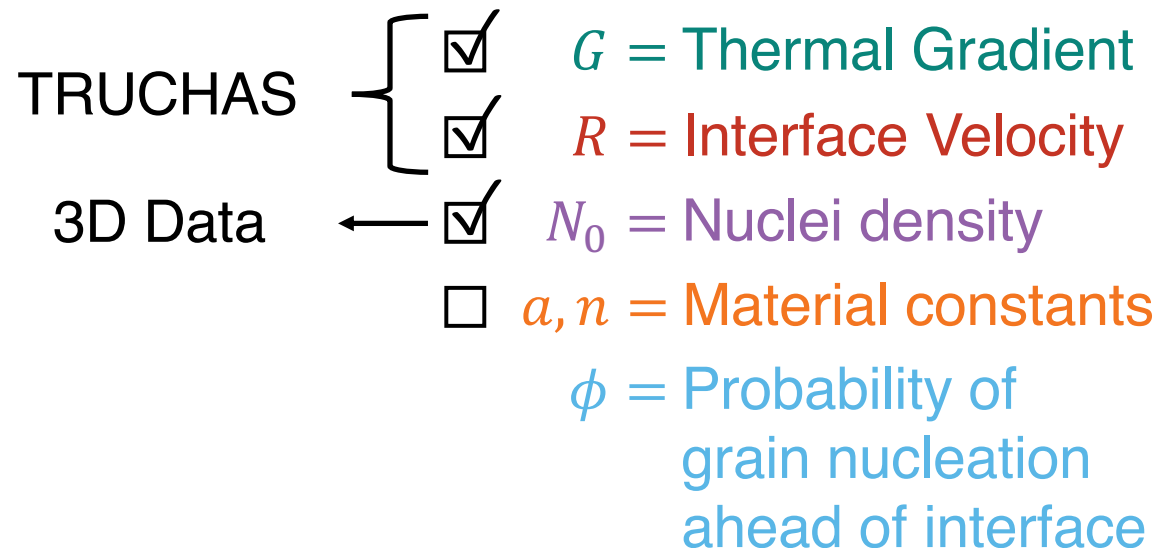
3D data shows  $N_0$  is three orders of magnitude lower  
 $2 \times 10^{15} \rightarrow 5.3 \times 10^{12} \text{ m}^{-3}$

ahead of interface

# Checklist for Columnar to Equiaxed Transition (CET) Model

- Want to predict the formation of nucleated grains

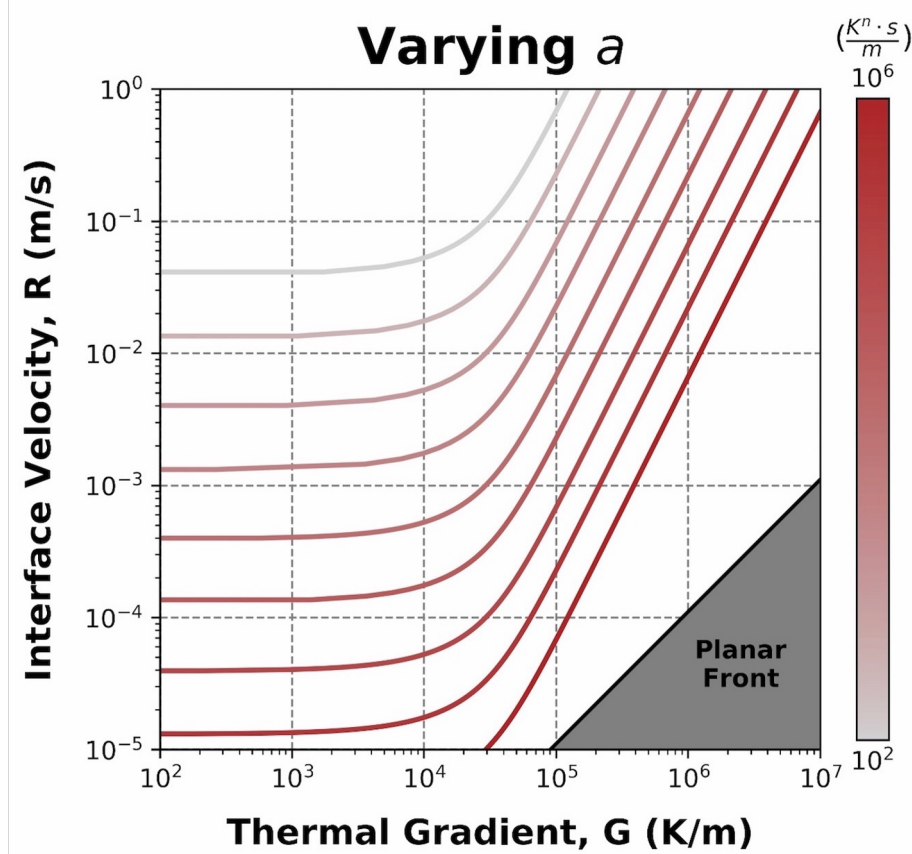
$$\phi = 1 - \exp \left\{ \frac{-4\pi N_0 a^{3/n}}{3(n+1)^3} \left( \frac{R}{G^n} \right)^{3/n} \right\}$$



# Checklist for Columnar to Equiaxed Transition (CET) Model

- Want to predict the formation of nucleated grains

$$\phi = 1 - \exp \left\{ \frac{-4\pi N_0 a^{3/n}}{3(n+1)^3} \left( \frac{R}{G^n} \right)^{3/n} \right\}$$

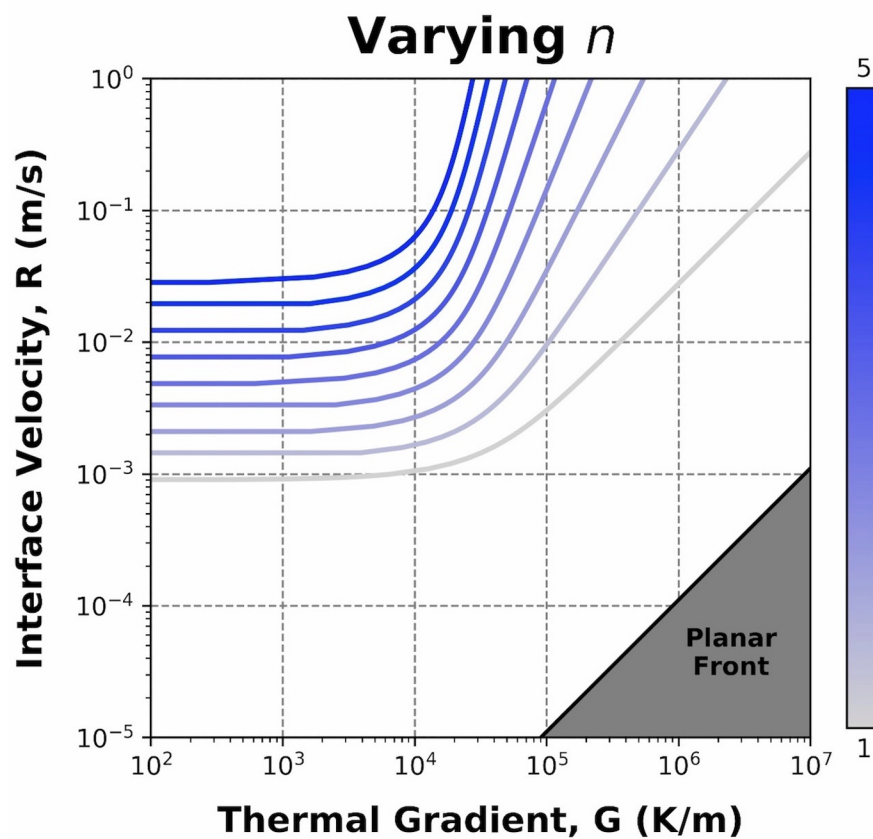


- $G$  = Thermal Gradient
- $R$  = Interface Velocity
- $N_0$  = Nuclei density
- $a, n$  = Material constants
- $\phi$  = Probability of grain nucleation ahead of interface

# Checklist for Columnar to Equiaxed Transition (CET) Model

- Want to predict the formation of nucleated grains

$$\phi = 1 - \exp \left\{ \frac{-4\pi N_0 a^{3/n}}{3(n+1)^3} \left( \frac{R}{G^n} \right)^{3/n} \right\}$$

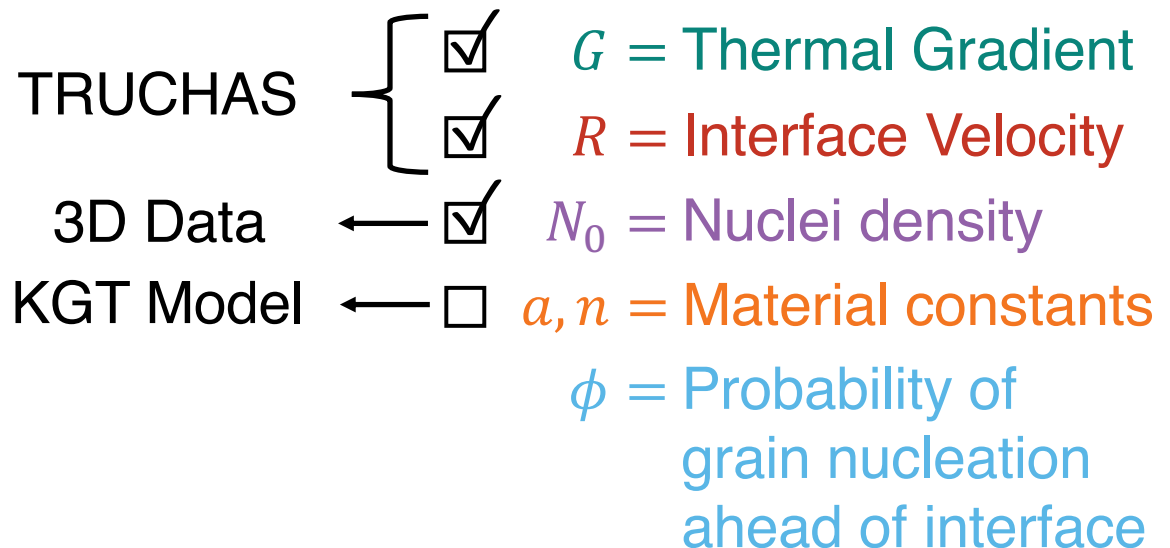


- $G$  = Thermal Gradient
- $R$  = Interface Velocity
- $N_0$  = Nuclei density
- $a, n$  = Material constants
- $\phi$  = Probability of grain nucleation ahead of interface

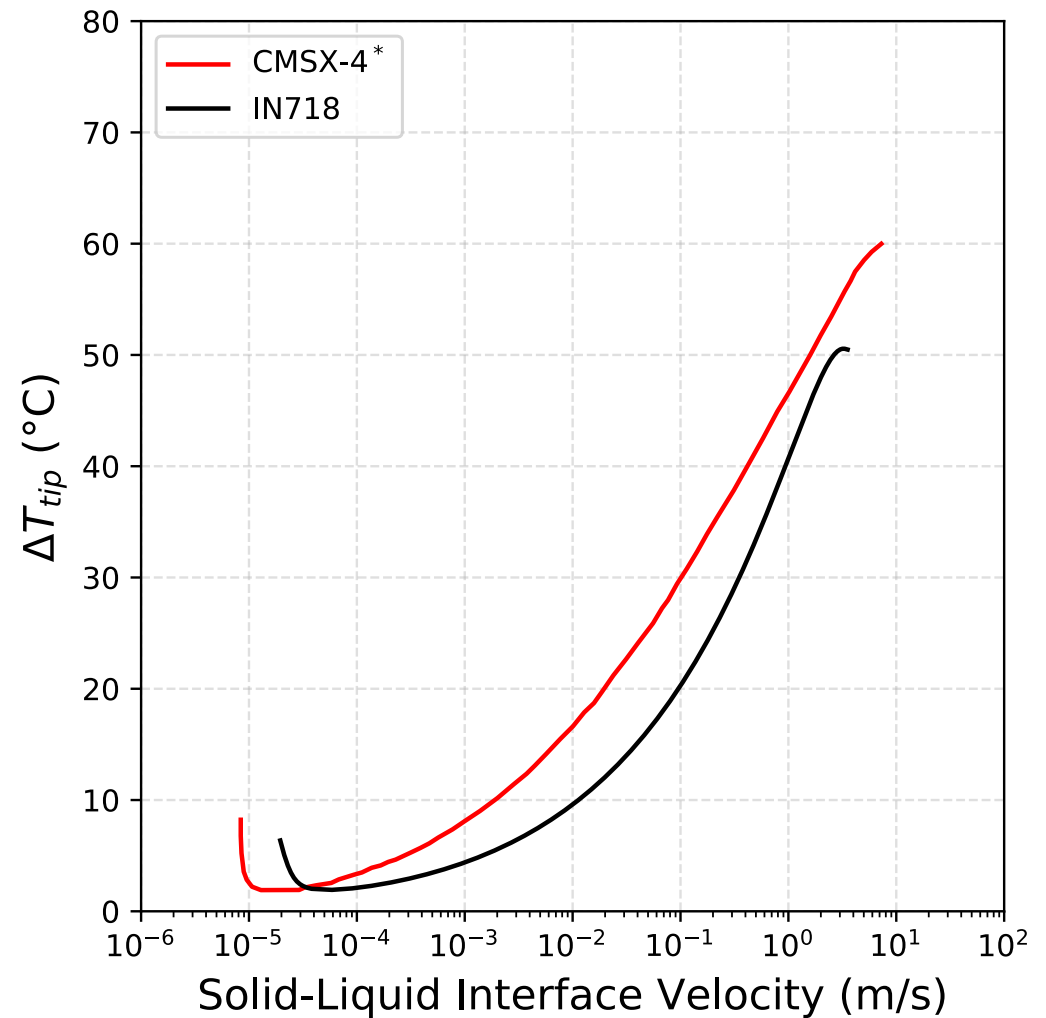
# Material constants are alloy dependent, but can be determined using KGT model

- Want to predict the formation of nucleated grains

$$\phi = 1 - \exp \left\{ \frac{-4\pi N_0 a^{3/n}}{3(n+1)^3} \left( \frac{R}{G^n} \right)^{3/n} \right\}$$

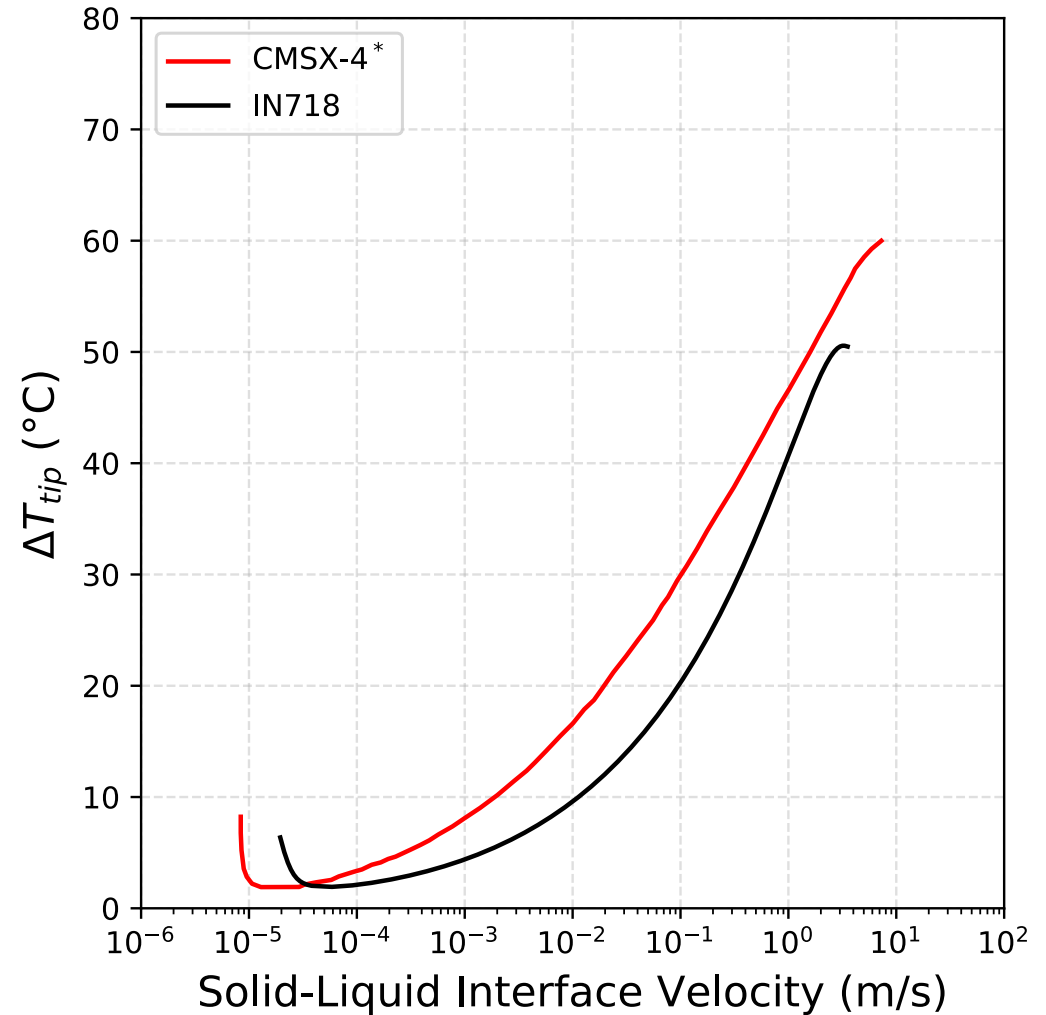


# Kurz Giovanola Trivedi (KGT) model predicts undercooling at the dendrite tip



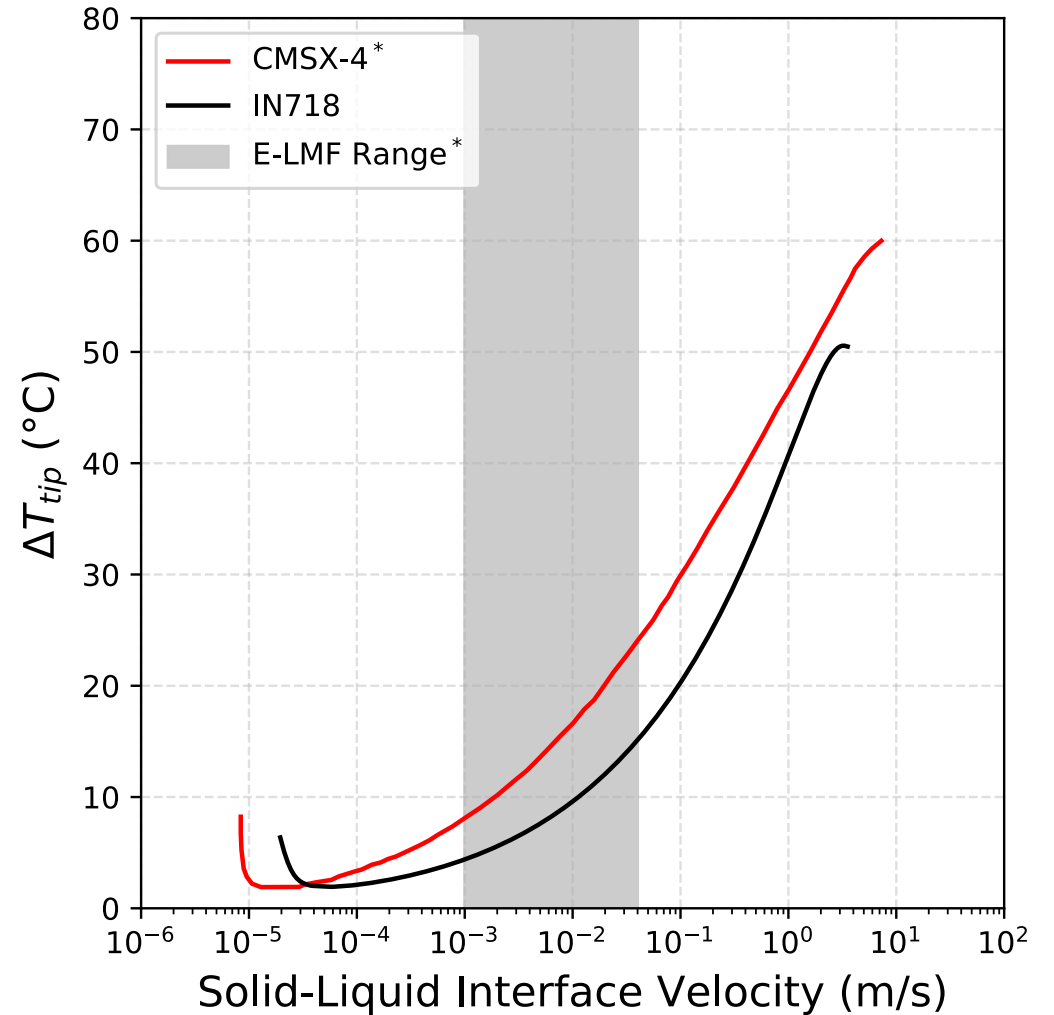
# Kurz Giovanola Trivedi (KGT) model predicts undercooling at the dendrite tip

$$\Delta T_{tip} = (a \cdot R)^{1/n}$$



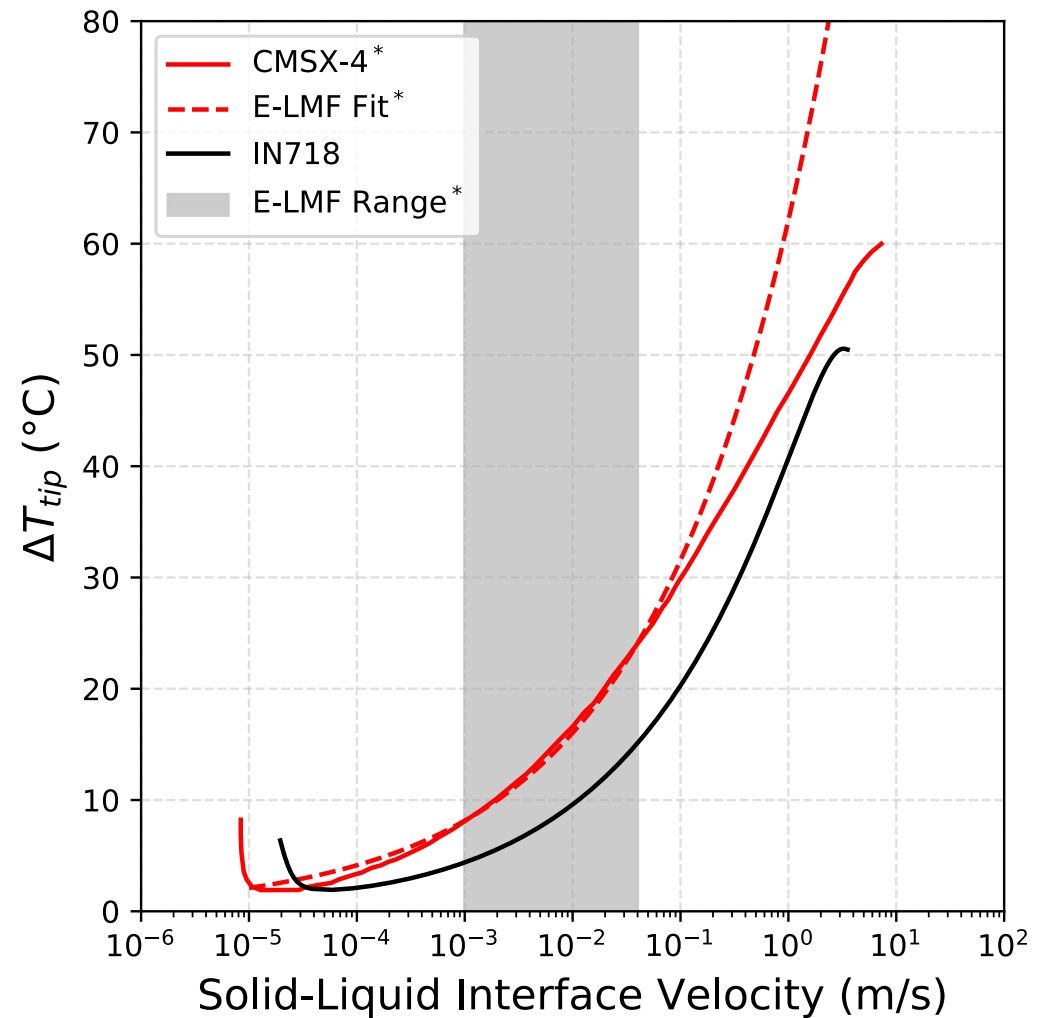
# Kurz Giovanola Trivedi (KGT) model predicts undercooling at the dendrite tip

$$\Delta T_{tip} = (a \cdot R)^{1/n}$$



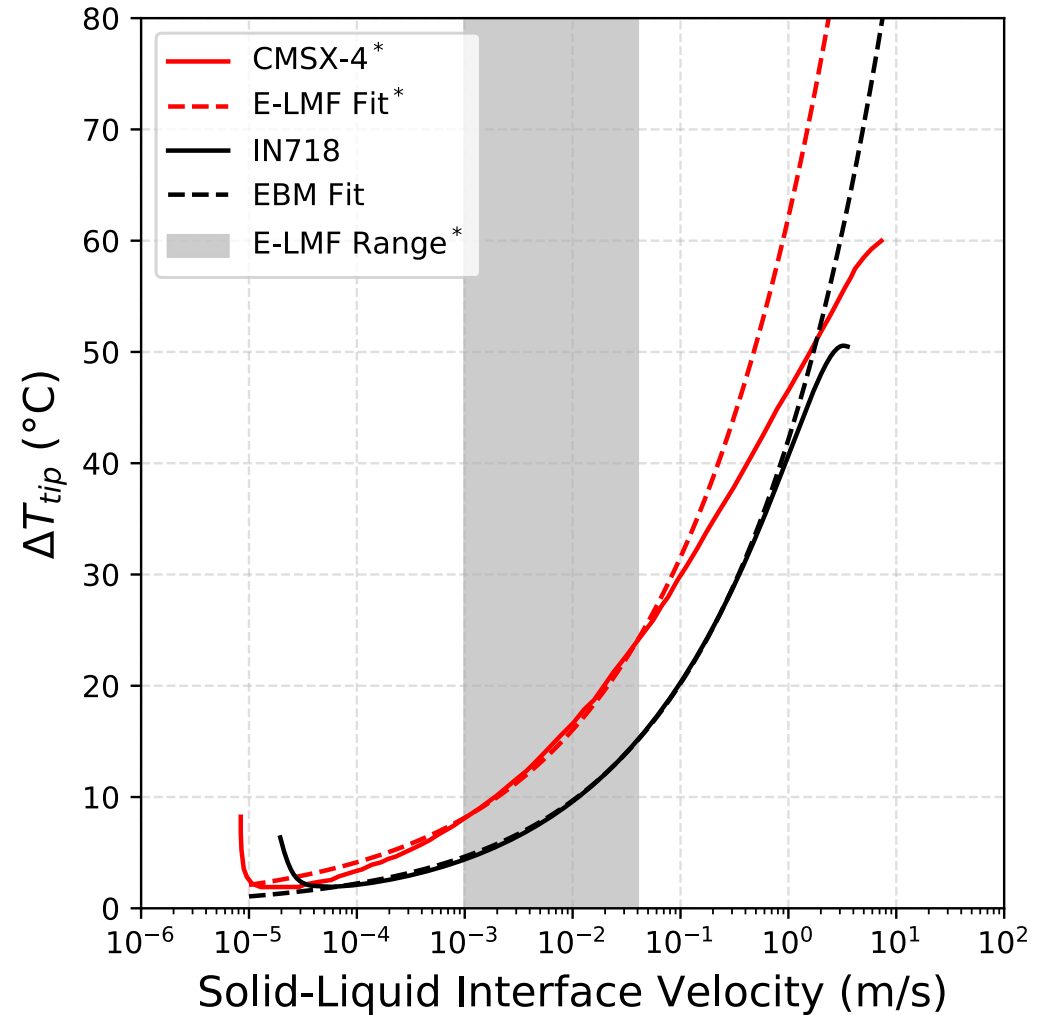
# Kurz Giovanola Trivedi (KGT) model predicts undercooling at the dendrite tip

$$\Delta T_{tip} = (a \cdot R)^{1/n}$$



# Kurz Giovanola Trivedi (KGT) model predicts undercooling at the dendrite tip

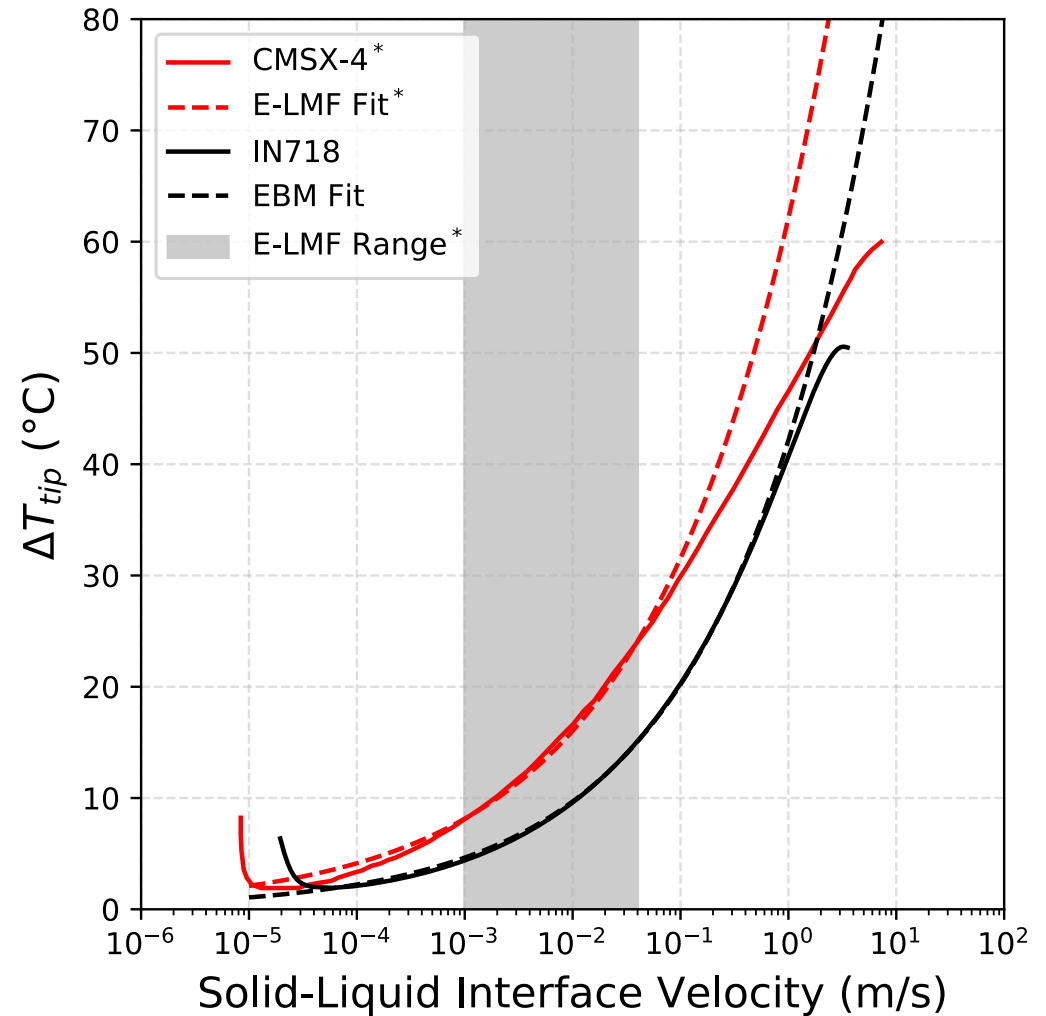
$$\Delta T_{tip} = (a \cdot R)^{1/n}$$



# Kurz Giovanola Trivedi (KGT) model predicts undercooling at the dendrite tip

$$\Delta T_{tip} = (a \cdot R)^{1/n}$$

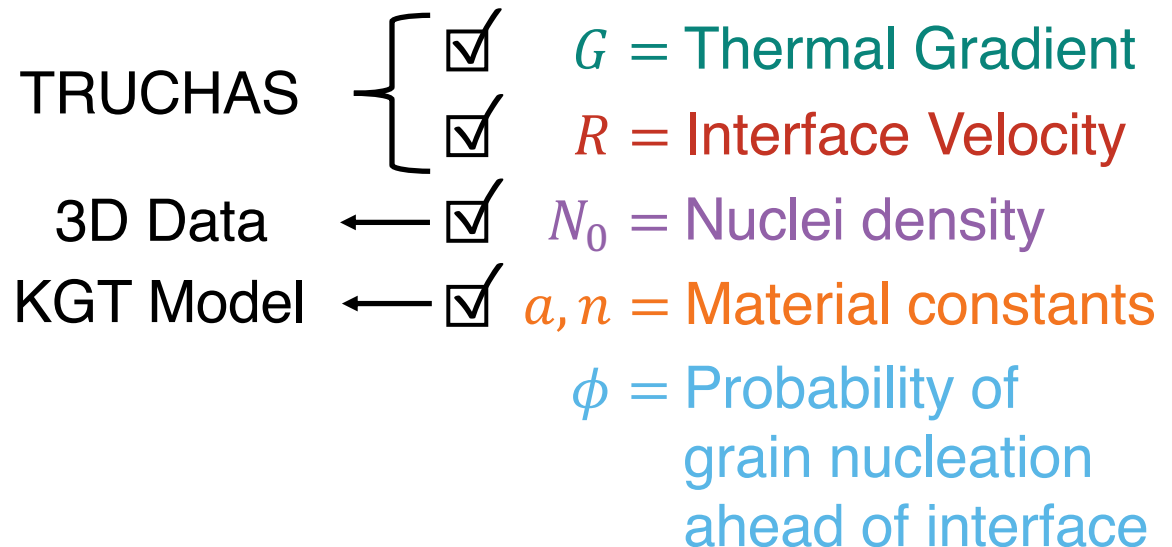
- $a$  decreases by an order of magnitude (smaller equiaxed processing window)  
 $1.25 \times 10^6 \rightarrow 1.23 \times 10^5$
- $n$  decreases (larger equiaxed processing window)  
 $3.4 \rightarrow 3.13$



# Checklist for Columnar to Equiaxed Transition (CET) Model

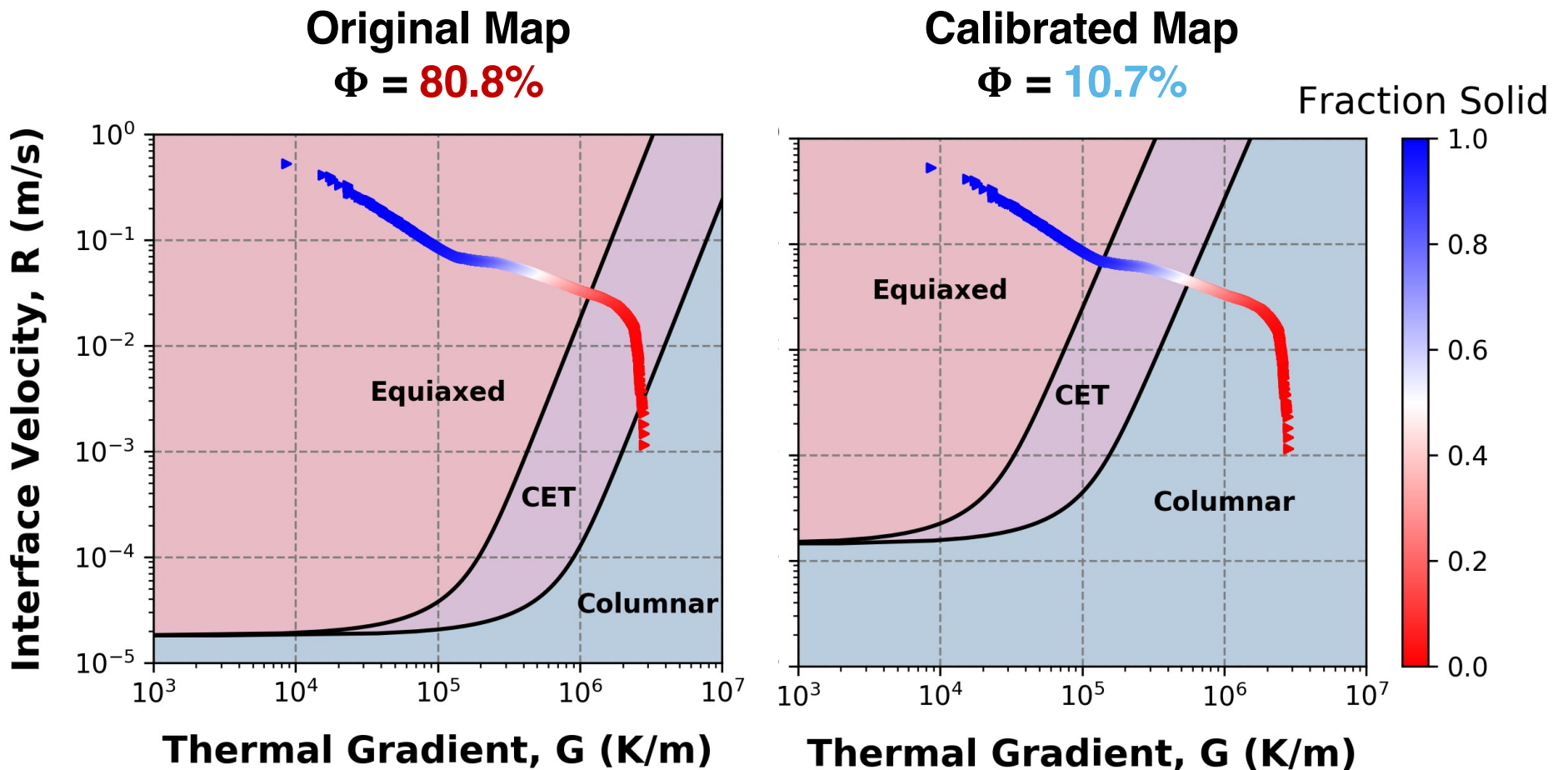
- Want to predict the formation of nucleated grains

$$\phi = 1 - \exp \left\{ \frac{-4\pi N_0 a^{3/n}}{3(n+1)^3} \left( \frac{R}{G^n} \right)^{3/n} \right\}$$



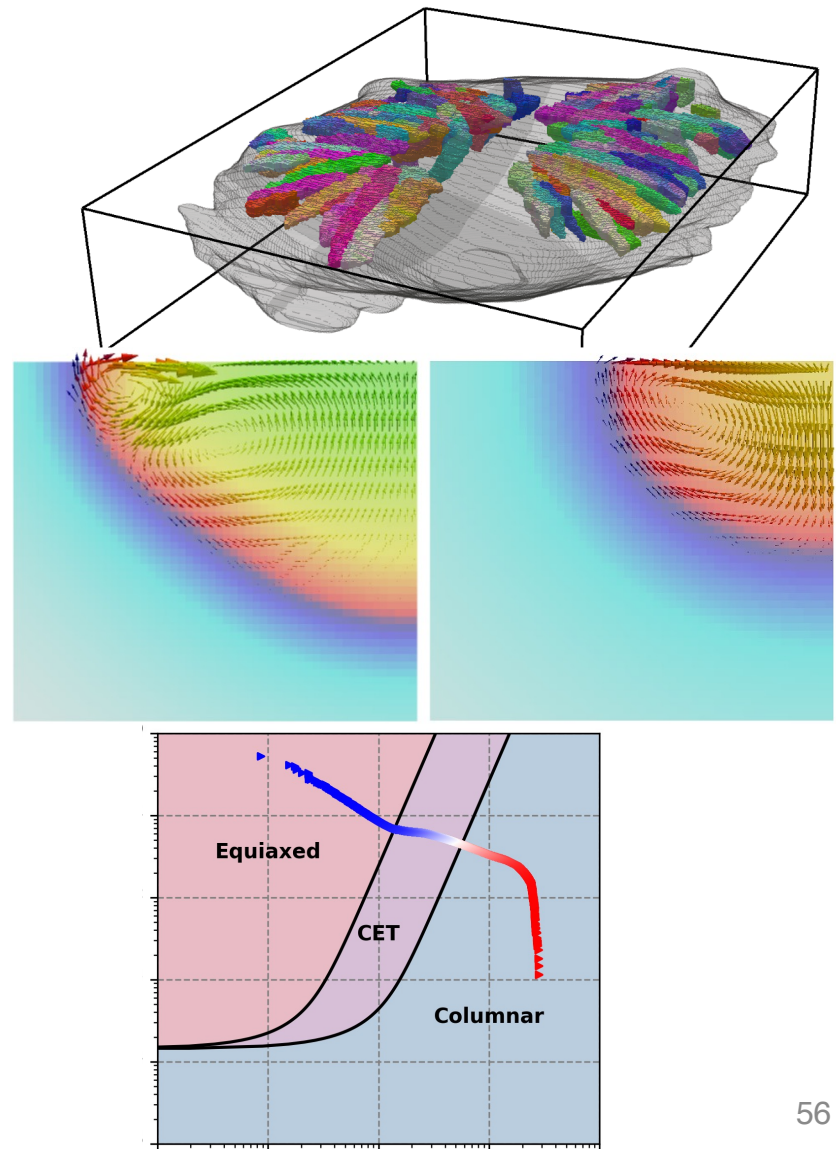
# Calibrated processing map accurately predicts microstructure

- Measured  $\Phi = 11.4\%$  from 3D data



# Summary

- 3D provides direct measurement of ground truth microstructures for calibration of processing maps
- Advanced simulations can provide insight to microstructure evolution during solidification
- Processing maps are alloy- and processing-dependent, and must be calibrated for the specific application of interest



# Thanks!

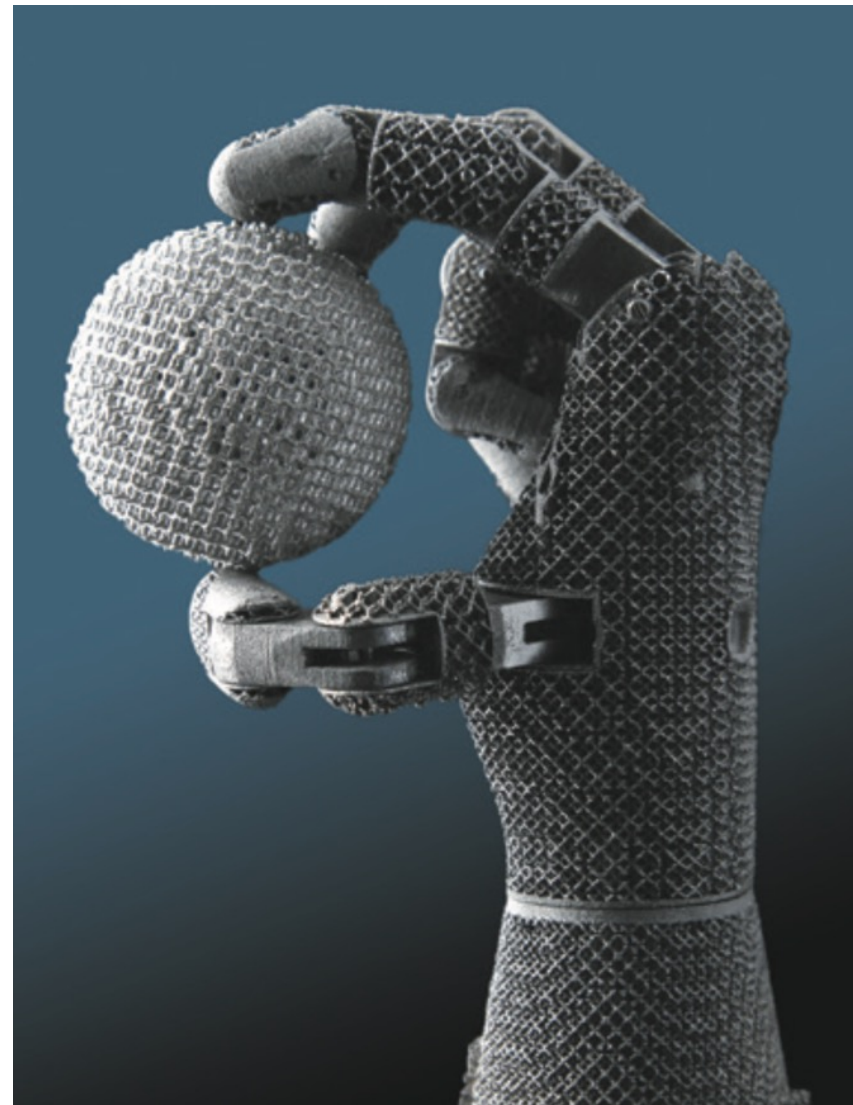


*Image courtesy ORNL MDF*